

Wind Power Meteorology

Lundtang Petersen, Erik; Mortensen, Niels Gylling; Landberg, Lars; Højstrup, Jørgen; Frank, Helmut Paul

Publication date:
1997

Document Version
Publisher's PDF, also known as Version of record

[Link back to DTU Orbit](#)

Citation (APA):
Lundtang Petersen, E., Mortensen, N. G., Landberg, L., Højstrup, J., & Frank, H. P. (1997). Wind Power Meteorology. Risø National Laboratory. Risø-I, No. 1206(EN)

DTU Library

Technical Information Center of Denmark

General rights

Copyright and moral rights for the publications made accessible in the public portal are retained by the authors and/or other copyright owners and it is a condition of accessing publications that users recognise and abide by the legal requirements associated with these rights.

- Users may download and print one copy of any publication from the public portal for the purpose of private study or research.
- You may not further distribute the material or use it for any profit-making activity or commercial gain
- You may freely distribute the URL identifying the publication in the public portal

If you believe that this document breaches copyright please contact us providing details, and we will remove access to the work immediately and investigate your claim.

Risø-I-1206(EN)

Wind Power Meteorology

Erik L. Petersen, Niels G. Mortensen, Lars Landberg,
Jørgen Højstrup and Helmut P. Frank

Risø National Laboratory, Roskilde, Denmark
December 1997

Abstract Wind power meteorology has evolved as an applied science, firmly founded on boundary-layer meteorology, but with strong links to climatology and geography. It concerns itself with three main areas: siting of wind turbines, regional wind resource assessment, and short-term prediction of the wind resource. The history, status and perspectives of wind power meteorology are presented, with emphasis on physical considerations and on its practical application. Following a global view of the wind resource, the elements of boundary layer meteorology which are most important for wind energy are reviewed: wind profiles and shear, turbulence and gust, and extreme winds.

The data used in wind power meteorology stem mainly from three sources: on-site wind measurements, the synoptic networks, and the re-analysis projects. Wind climate analysis, wind resource estimation and siting further require a detailed description of the topography of the terrain – with respect to the roughness of the surface, near-by obstacles, and orographical features. Finally, the meteorological models used for estimation and prediction of the wind are described; their classification, inputs, limitations and requirements. A comprehensive modelling concept, meso/micro-scale modelling, is introduced and a procedure for short-term prediction of the wind resource is described.

This manuscript has been submitted for publication in two parts in *Wind Energy*, published by John Wiley & Sons Ltd. Part I, *Climate and Turbulence*, covers Sections 1–4 of the present report and Part II, *Siting and Models*, Sections 5–7.

Contents

1 INTRODUCTION	4
2 HISTORY, STATUS & PERSPECTIVES	5
2.1 Physical considerations	5
3 WEATHER AND WIND CLIMATE	10
3.1 Wind climates of the World	11
3.2 Climate variability and change	12
4 WINDS IN THE ATMOSPHERIC BOUNDARY LAYER	13
4.1 Wind profiles and shear	13
4.2 Turbulence and gusts	16
4.3 Extreme winds and exceedance statistics	21
5 WIND CLIMATE DATA SOURCES	23
5.1 Re-analysis projects	23
5.2 The synoptic network stations	23
5.3 On-site wind measurements	24
6 TOPOGRAPHY	27
6.1 Surface roughness	27
6.2 Obstacles	30
6.3 Terrain orography	30
7 METEOROLOGICAL MODELS	32
7.1 Input to models	32
7.2 Classifications of models	33
7.3 Limitations of and requirements to models	33
7.4 Combined meso/micro-scale modelling	34
7.5 Short-term prediction	35
8 AREAS OF FURTHER RESEARCH	38

1 INTRODUCTION

Wind Power Meteorology is not a term to be found in a standard glossary of meteorological terms. However, it is a discipline which has evolved under its own provisions. It can formally be described as applied geophysical fluid dynamics, but a more understandable definition would rest on a combination of meteorology and applied climatology. Meteorology is atmospheric science in its widest sense. It consists of the atmospheric thermodynamics and chemistry, the qualitative and quantitative description of atmospheric motion, and of the interaction between the atmosphere and the Earth's surface and biosphere in general. Its goals are the complete understanding and the accurate prediction of atmospheric phenomena. It is one of the most complex fields of both natural and applied science. Climatology is the scientific study of climate and its practical application. It uses the same basic data as meteorology and the results are particularly useful to problems in industry, agriculture, transport, building construction, and biology. Many of the aspects of climatology make it a part of meteorology, but when the emphasis is on specific climate conditions at a particular point on the Earth's surface, it is clearly part of geography. Wind power meteorology thus does not belong wholly within the fields of either meteorology, climatology or geography. It is applied science, whose methods are meteorological, but whose aims and results are geographical. It concerns itself with three main areas: micro-siting of wind turbines, estimation of regional wind energy resources, and short-term prediction of the wind power potential, hours and days ahead.

With respect to wind power meteorology, *siting* is defined as estimation of the mean power produced by a specific wind turbine at one or more specific locations. A full siting procedure includes considerations such as the availability of power lines and transformers, the present and future land use, and so on. However, these aspects are not considered here. To put 'paid' to the problem of proper siting of wind turbines with respect to the wind resource, we require proper methods for calculating the wind resource, the turbulence conditions, the extreme wind conditions, and the effects of rotor wakes.

Regional assessment of wind energy resources means estimating the potential output from a large number of wind turbines distributed over the region. Ideally, this results in detailed, high-resolution and accurate resource maps, showing the wind resource (yearly and seasonal), the wind resource uncertainty, and areas of enhanced turbulence.

Forecasting of the meteorological fields, hours and days ahead is one of the great challenges of meteorology. The tremendous increase in computer power and of the observational density (by satellites in particular) and quality have contributed to a marked increase in forecasting skills over the last decade. This, in turn, has made it possible to construct a methodology by combining numerical weather prediction models with micro-siting models to predict the power output from specific wind farms up to 48 hours ahead.

These three topics and wind power meteorology in general are treated in the following sections. First, the history, status and perspectives are described. This description constitutes by no means a full account of what has been done by whom; admittedly, it gives a rather subjective view: the Risø perspective on matters. The next two sections set the stage for wind power meteorology with respect to meteorology and climatology and the following section relates it to geography. Then wind data are treated, in particular the means by which these data are obtained. Finally, a description of the numerical meteorological models – spanning from full, global circulation models over high-resolution limited-area models to micro-scale models – is given.

2 HISTORY, STATUS & PERSPECTIVES

The discipline Wind Power Meteorology has evolved together with the commercial evolution of the wind turbine and the large-scale utilization of wind for electricity generation. From the early seventies, groups world-wide began to work with meteorological and climatological questions related to wind energy and numerous publications can be found in the literature. The national wind energy programs, which were initiated in a number of countries in the seventies, typically included national wind resource surveys. Among these, probably the best known are the Wind Energy Resource Atlas of the United States by Pacific Northwest Laboratory [1] and the Wind Atlas for Denmark by Risø National Laboratory [2], both published in 1980. In addition to these atlases a number of so-called siting handbooks were produced; most notably in the USA (1977) [3] and (1980) [4], in Canada (1984) [5], and in the Netherlands (1986) [6]. The Danish Wind Atlas and later the European Wind Atlas (1989) [7] serve both purposes, as wind resource atlas and siting handbook.

During the 1980s wind turbine development increased dramatically, and large demonstration wind turbines were erected and tested, but often dismantled after a few years of operation due to unsuccessful design. In the meantime, the small and privately produced turbines went on growing larger and more reliable and – thanks to various political initiatives – a sometimes turbulent market was created. Best known is the growth of the European and American wind turbine industry; the eruption of the Californian market and the subsequent decline leading to multiple bankruptcies for the industry. Following this incidence a slower, but consolidate growth of the European market developed: the wind energy community had learned its lesson from the Californian adventure. The importance of an accurate knowledge of the overall wind resource and reliable methods for the siting of wind turbines had become increasingly clear.

Through the 1990s the world has seen a continuous growth in the application of wind energy. The competition has become fierce, not only between specific brands of turbines, but also between projects demanding large investments. Which project to select and on what grounds? Usually, economy and, consequently, the expectation to the power production during the lifetime of the wind turbine are crucial parameters. Here, the application of wind power meteorology plays an ever increasing important role. It is interesting to note that this discipline has evolved over the last 20 years or more, turning a relatively ‘free’ academic discipline into ‘hard core’ research and development under the pressure from the wind energy community – with a strong and almost unrealistic demand for accurate and efficient methods. Many of the early methods put forward did not survive. The methods that are left are in return extensively used. With the wisdom of hindsight it is straightforward to explain what happened, why it happened and finally in what direction the development must go. The answer lies in the physics: the more relevant physics that can be implemented in the methods, the more general and realistic the models and the more accurate and reliable the results. In the following, we will go through simple physical arguments in support of this allegation.

2.1 Physical considerations

The state of the atmosphere is well described by seven variables: pressure, temperature, density, moisture, two horizontal velocity components, and the vertical velocity; all functions of time and position. The behavior of these seven variables is governed by seven equations: the equation of state, the first law of thermodynamics, three components of Newton’s second law, and the continuity equations for

mass and water substance. These equations are mathematical relations between each atmospheric variable and their temporal and spatial derivatives. Mathematical models of the atmosphere can be obtained by integrating the relevant equations with special initial and boundary conditions. The equations can be solved numerically by forward marching in time, using the time rates of change of the variables; the derivatives are replaced by ratios of finite differences, and changes of the variables over a certain time interval are computed repeatedly as long as needed.

The atmosphere contains motions with scales varying from about 1 mm to thousands of kilometers. Ideally, mathematical models should be constructed from observations with one millimeter spatial and with a fraction of a second temporal resolution. Clearly, this is impossible in practice, and models are constructed separately for systems on different scales. Thus, for example, there are models for local circulations such as sea breezes, for flow over mountains, for weather developments over Europe, or for the entire globe. Depending on the system modelled, the equations can be simplified and for the development of wind power meteorology the starting point is the simplest model for motion in the atmosphere: steady winds over very extensive plains under an overcast sky or, in other words: a stationary wind field over an infinite flat plane of uniform roughness with neutral stratification. The only quantity of interest is the variation of wind speed with height. Straightforward physical considerations [2, 8] lead to the well-known logarithmic wind profile, which is determined solely by three variables: the height above ground, the roughness length and the friction velocity. The roughness length parameterizes the roughness of the surface and the friction velocity parameterizes the frictional force between the moving air and the ground.

From the starting point of the infinite plate at rest, we move to the rotating earth. Far away from the ground, the atmosphere can not feel the friction and the flow is in equilibrium with the pressure force and the Coriolis force. The latter is caused by the rotation of the Earth. The resulting wind is called the geostrophic wind. Moving down to the surface, the wind changes from geostrophic speed to zero speed at the height of the roughness length. At the same time the wind direction changes, rotating anti-clockwise on the northern hemisphere and clockwise on the southern hemisphere. The balance between the forces can be derived theoretically under the idealized conditions of stationarity, homogeneity and barotropic stratification (the pressure gradient being constant over the depth of the boundary layer). For the conditions of neutral stability, the balance can be expressed as a relation – the geostrophic drag law – between the surface friction velocity and the geostrophic wind, with the roughness length and the Coriolis force as parameters, see Eq. (3). The geostrophic wind can be calculated from the surface pressure gradient and is often close to the wind speed observed by radiosondes above the boundary layer. The combination of the logarithmic wind profile and the geostrophic drag law provides us with an easy-to-handle model atmosphere: the Coriolis parameter is known for a given location and the roughness length can be estimated from the characteristics of the ground cover. Hence, if we can determine the geostrophic wind, the friction velocity can be calculated from the drag law and, in turn, applied in the logarithmic profile to calculate the wind speed at a desired height.

Now we introduce weather and climate; the atmosphere is no longer assumed stationary, but characterized by ‘synoptic’ activity, i.e. the passing of high and low pressure systems. The geostrophic wind has a climatological variation, which we need to estimate in order to get the climatology of the surface wind. This was the philosophy behind the Danish Wind Atlas work (1977-80) [2]. Surface pressure data measured every third hour over 13 years at 55 stations in Norway, Sweden, Denmark, Germany, and Poland, were used to calculate a 13-year time-series of the

geostrophic wind over Denmark. This was then used to calculate time-series of the surface wind at heights between 10 and 200 meters, for four values of the roughness length. Each value of the roughness length was assigned to a characteristic type of terrain, named a roughness class. Initially, the aim of the project was to produce maps over Denmark of the wind resources. Early in the project it became clear, that in order for such maps to make any sense they would have to be produced with an – at that time – impossible high resolution. The reason for this is the dramatic variation of the wind conditions which, due to the extreme dependence of the wind speed on the topographical features, can be experienced near the surface over short distances. Instead of producing maps, a method which could be used to produce maps of high resolution at particular locations was developed. More specifically, the method, which later became known as the Wind Atlas Method, was created such that a user, having specified the roughness classes in each of eight direction sectors (N, NE, ..., NW), could use the tables and graphs in the Atlas to calculate the distribution function of the wind at the desired height. This was before the advent of the PC.

One of the assumptions used in the development of the wind atlas method was that the distribution of wind speeds is well approximated by the Weibull distribution function. Several investigations before the Atlas had hinted at this and the general experience today is that well-measured data at locations with moderate to high winds almost always can be approximated by the Weibull function. The time-series of the geostrophic wind calculated from the pressure data had a near-perfect Weibull distribution as shown in Fig. 1(a). The distribution functions of the surface wind speed time-series, calculated as described above, were then fitted with the Weibull distribution and the resulting two parameters describing the distribution, the scale parameter A and shape parameter k , were plotted for five heights, four roughness classes and eight direction sectors. A typical graph is shown in Fig. 1(b). More than 6000 wind turbines operating in Denmark and Germany have been sited using this method, hence there is an immense amount of experience behind its use.

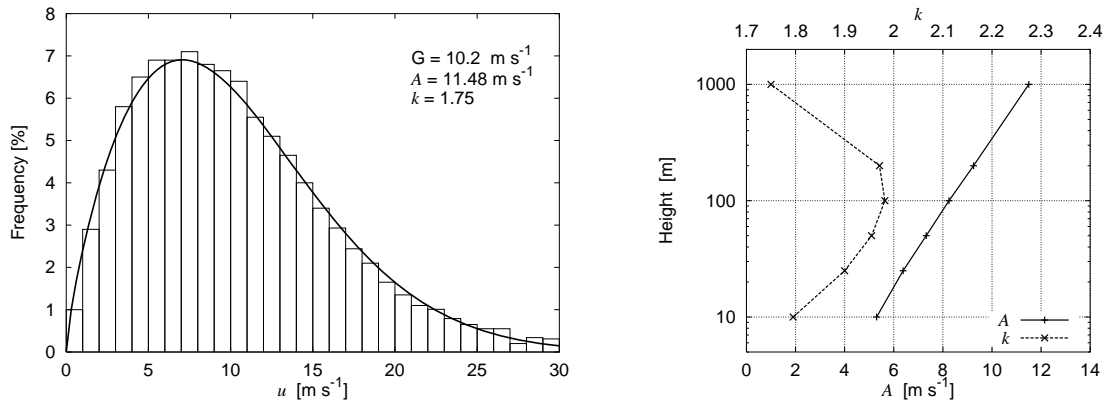


Figure 1. (a) The distribution of the geostrophic wind over Denmark [2]. (b) Weibull A - and k -parameters as functions of height over roughness class 2 [2]. The values shown at 1000 m correspond to the geostrophic wind.

In the construction of the Danish Wind Atlas it was necessary to move a step away from the idealized world. It was essential to include the effects of changes from one roughness class to another and from height variations in the terrain. In other words, it was inevitable to construct models which, on the basis of simple information extracted from standard topographical maps, could calculate the

effect on the wind from topographical features. This was achieved by combining contemporary theories with experimental investigations. The Atlas contains a method for calculating the effect of a change of roughness class, the so-called roughness change model, and a model for calculating the speed-up which occurs when the flow passes over a hill, the so-called hill model. Further, it was necessary to construct a model for the effect of sheltering obstacles in the terrain, such as houses and shelter belts, the so-called shelter model.

In 1981, the European Commission launched its first wind energy research program. In the plans was the creation of a European wind atlas, based on the Danish Wind Atlas methodology for non-mountainous terrain and an application of a mass-consistent model for mountainous terrain. An assembled working group immediately deemed this approach impossible. Not only was the necessary collection of pressure data prohibitively immense, but so were also the requirements for computer power. Furthermore, the influence on the pressure measurements from the actual heights of the synoptic stations above mean sea level could introduce so large errors in the calculation of the geostrophic wind that the resulting statistics most likely would be useless. The use of a mass-consistent model for the mountainous areas had the problem that because the physics is extremely simplified – basically only the continuity equation – it requires a network of measurements with an unrealistic density. Therefore a methodology was established in which the first step was to give a systematic description of the various types of landscapes in Europe and the next to provide methods and data to be used in each landscape type. Five distinct landscape types were recognized and the topography and wind climatology were described. For the creation of the European Wind Atlas the strategy was to adapt parts of the methodology from the Danish Wind Atlas for the relatively simple landscapes, and for the complex landscapes to collect as many high-quality wind records as possible and develop a method to describe and classify the stations in a unified way.

As mentioned above, the Danish method could not be used straightforwardly because of the insurmountable difficulties in the pressure analysis. Instead, another method was put forward: the double vertical and horizontal extrapolation method. The idea behind this is quite simple: if we have measured the wind speed at a height of 10 meters at one station and we are able to estimate the distribution of the roughness length around the station, then we can find the friction velocity from the logarithmic profile and apply this in the geostrophic drag law to calculate the geostrophic wind. Having determined the geostrophic wind this way, we can proceed as in the Danish Wind Atlas method to calculate the Weibull statistics. And these statistics can then be used to estimate the wind statistics at specific locations up to 200 m a.g.l. The procedure is illustrated in Fig 2.

However, with the introduction of the double extrapolation method, the assumption about the uncomplicated neutral atmosphere had to be relaxed. This is so, because the climate of the surface heat flux is an important parameter for the vertical extrapolation of the wind distribution with height. Even at moderate wind speeds, deviations from the logarithmic profile occur when the height exceeds a few tens of meters. Deviations are caused by the effect of buoyancy forces in the turbulence dynamics; the surface roughness is no longer the only relevant surface characteristic, but has to be supplemented by parameters describing the surface heat flux. With cooling at night, turbulence is lessened causing the wind profile to increase more rapidly with height; conversely, daytime heating causes increased turbulence and a wind profile more constant with height. In order to take into account the effects of the varying surface heat flux without the need to model each individual wind profile, a simplified procedure was adopted which only requires the climatological average and root-mean-square of the surface heat flux. This procedure introduces the degree of ‘contamination’ by stability effects

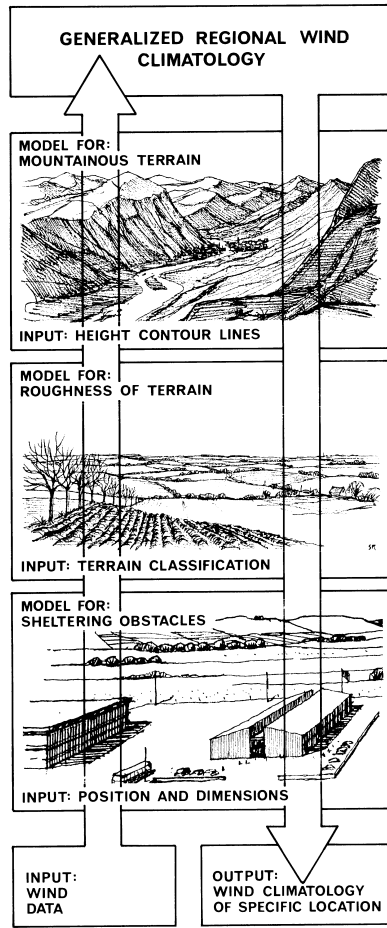


Figure 2. The wind atlas methodology used for the European Wind Atlas [9]. Meteorological models are used to calculate the regional wind climatologies from the raw data. In the reverse process – the application the Wind Atlas – the wind climate at any specific site may be calculated from the regional climatology.

to the logarithmic wind profile when conditions at different heights and surfaces are calculated.

Owing to the complexity of the European landscape and the large number of stations used for the analysis, it was necessary to replace the roughness change model and the hill model by much more general computerized models, which were able to handle topographical map information in digital form. These models had to be developed, verified and applied. The result was a flow-over-hill model with an expanding polar grid centered at the point of interest, enabling a very detailed description of the terrain around a specific location. Because the terrain elevations closest to the location exert the strongest influence, this is a very much desired feature. The roughness change model was initially expanded to multiple roughness changes and subsequently developed into a more general model, capable of handling roughness areas extracted directly from topographical maps. The European Wind Atlas was published in 1989, one year after the calculational methods had been made publicly available in the PC-program WASP: the Wind Atlas Analysis and Application Program [9]. Subsequently, a number of similar studies were undertaken in e.g. Norway (1987) [10], Jordan (1989) [11], Western Australia (1990) [12], Switzerland (1990) [13], Algeria (1991) [14], Finland (1994) [15], Sweden (1995) [16], Germany (1996) [17], Egypt (1996) [18], and similar efforts are in

progress in Libya, Syria, Russia and elsewhere.

The primary use of WASP has been for siting of wind turbines world-wide, single or in farms. Over the decade it has been in use, it has developed into a generally accepted standard for micro-siting. However, it has its well-recognized limitations: the more complicated the situation is with respect to topography, climatology, or both, the more uncertain are the results from the calculations. Many of the procedures that constitute the method are strictly applicable only under an idealized and limited range of conditions. The most severe problems are encountered in mountainous terrain where large-scale effects render the model increasingly deficient because of the importance of dynamics which is at present not accounted for in the model. The only way forward is to use more complete physical models. The next level consists of the so-called meso-scale models. They build on the full set of equations and are therefore – formally – capable of modelling all types of flow in complex situations. Their disadvantage lies in the difficulties encountered in prescribing the initial and boundary conditions accurately. Furthermore, they typically model an area of the order of $100 \times 100 \text{ km}^2$ with a resolution of 5–10 km. To zoom in on specific locations, it is necessary to apply a high-resolution model like WASP. This line has been followed in a number of studies [19]. The European Wind Atlas work was followed up by the EU Commission with a study called ‘Measurements and modelling in complex terrain’ [20]. The aim was to be able to calculate the available wind resources in mountainous terrain with an acceptable low uncertainty. The project encompassed model development and measurements in several mountainous regions of Europe for verification and demonstration. The result is produced by a combination of the Karlsruhe Atmospheric Mesoscale Model (KAMM) and WASP.

The perspectives for further progress of wind power meteorology are good: the ever-increasing computer power and efficiency of numerical methods allow for continuous development of the models involved, and the public availability of large databases on long-term global wind climatology and high-resolution topography (orography and land use) allows for production of world-wide reliable wind atlas data and for accurate siting of wind turbines.

3 WEATHER AND WIND CLIMATE

It is the wind in the lowest part of the atmosphere that is the most important atmospheric variable for wind power meteorology. During this century a scientific discipline named *boundary layer meteorology* evolved with the aim of describing the atmospheric processes in the atmospheric boundary layer. The application of this discipline has mainly been aimed at the study of air pollution, agriculture and wind engineering. Wind power meteorology has been fortunate to be able to draw from the acquired knowledge of boundary layer meteorology and until recently it is fair to say that wind turbine designers have not been able to make full use of it. However, this has now changed and the requirement for detailed and highly realistic models, for example a three-dimensional quantitative description of the turbulence over a rotor plane, is a tremendous challenge to wind power meteorology.

The atmospheric boundary layer is the layer of air directly above the earth’s surface. The layer extends to about 100 m above the ground on clear nights with low wind speeds, and up to more than two kilometers on a fine summer day. The lower part of this layer is called the surface layer and it is sometimes defined as a fixed fraction, say 10% of the boundary layer depth. For the purpose of climatology relevant to wind power utilization, we can often neglect the lowest wind speeds,

so situations where the atmospheric boundary layer extends to approximately one kilometer are of primary concern. It is in the lowest 100 m – the surface layer – that the logarithmic law for the wind profile and other relations described in the next section apply.

The wind profile we observe at any particular time is one measure of the elements of the current weather. If we continue to observe the same wind profile over years, we make up its *climatology*. It is worth-while for discussions ahead to reproduce here the generally accepted definitions of weather and climate [21]:

Weather is the totality of atmospheric conditions at any particular place and time – the instantaneous state of the atmosphere and especially those elements of it which directly affect living things. The elements of the weather are such things as temperature, atmospheric pressure, wind, humidity, cloudiness, rain, sunshine, and visibility.

Climate is the sum total of the weather experienced at a place in the course of the year and over the years. Because the average conditions of the weather elements change from year to year, climate can only be defined in terms of some period of time – some chosen run of years, a particular decade or some decades.

3.1 Wind climates of the World

The climate varies greatly around the globe. We are not concerned here with other elements than the wind and the wind resource, but note in passing that other climate elements, such as humidity, precipitation, temperature, and also average concentrations of particles, sea spray, etc. would be required for other purposes. An example of this is a ‘Corrosion Atlas’, which would be an appropriate thing for a wind turbine designer to have.

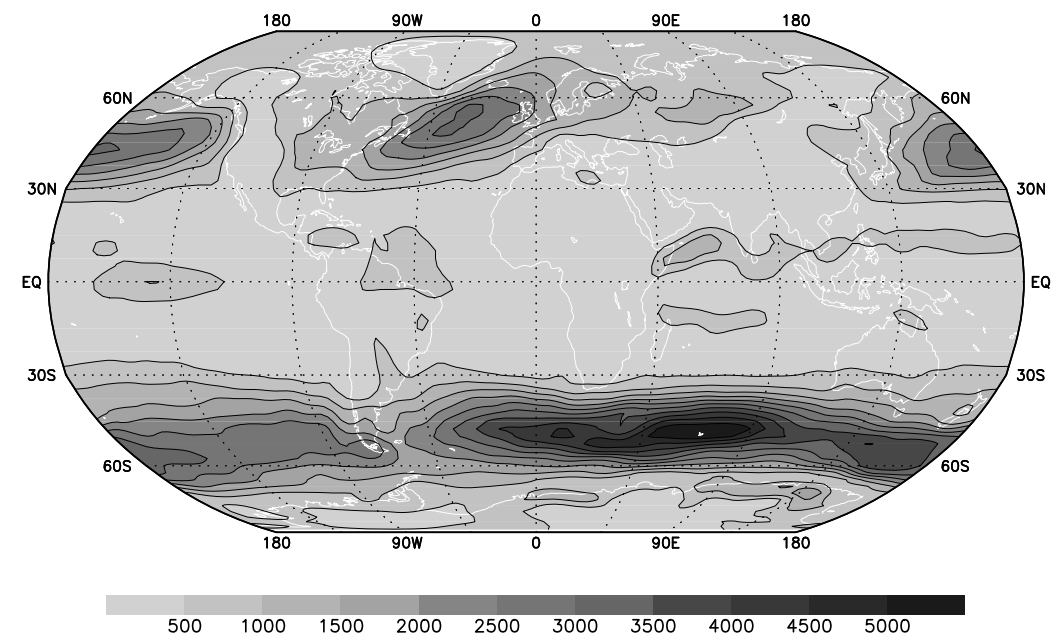


Figure 3. Energy flux of the wind at 850 hPa (≈ 1500 m a.s.l.) in Wm^{-2} from 8 years of the NCEP/NCAR reanalysis. The energy was calculated for every 2.5 deg. of latitude/longitude using an air density of 1.225 kg m^{-3} (figure created using the GrADS software by Brian Doty).

An overview of the global wind climate is illustrated in Fig. 3, where the mean wind-energy flux at 850 hPa (≈ 1500 m a.s.l.) is shown. The picture is a familiar one, displaying clearly the ‘roaring forties’ on the Southern Hemisphere and the extratropical cyclonic activity over the Northern Atlantic and the Northern Pacific. Furthermore, the southwest monsoon can be seen, with the Somali Jet standing out.

Evidently, this is a very coarse picture of the wind regimes of the World: it does not display local wind systems on scales less than a few hundred kilometers and larger-scale systems with strong yearly variations are suppressed, too. For a detailed description of the global climate, see [22, 23]. However, as a starting point for regional wind resource estimation world wide, the database used for the map is extremely useful in combination with adequate meteorological models.

The wind climatological description and classification of a particular location is not a simple matter. Many different types of wind statistics could be considered for a description of wind climates; local or regional. For the European Wind Atlas a graphical representation called the *wind climatological fingerprint* was developed [7]. Experience has shown that the collective information in the various statistics usually provides a good representation of the wind climate. Figure 4 elucidates the usefulness of parts of the fingerprint characterization; three widely different wind climates from the arctic, the Westerlies, and the trade winds are shown. The dramatic differences between these climates are obvious, especially for the yearly and the daily variations.

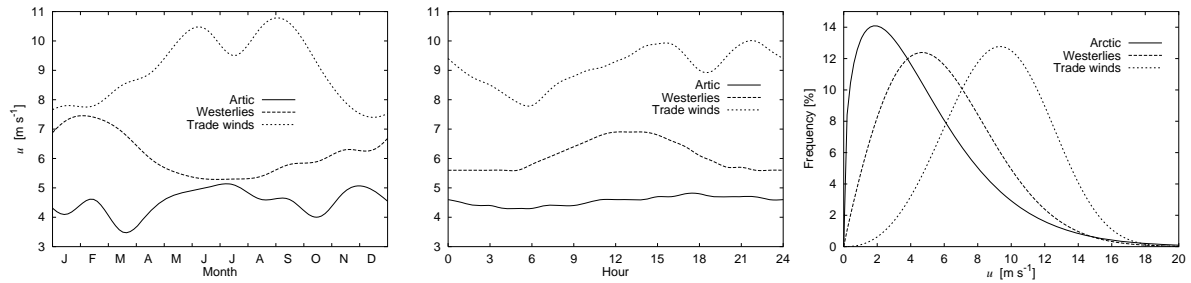


Figure 4. (a) Yearly and (b) daily variations of the mean wind speed for three different wind climates. (c) Frequency distributions of the wind speed at the same three locations.

3.2 Climate variability and change

Variability is an intrinsic feature of climate because the weather changes from year to year and between consecutive decades. The data which form the basis of any wind resource study cover a limited period of time, which in many cases is about ten years. The question therefore arises: to what extent is that period representative for the longer-term climate and, more importantly, how large a deviation must be expected in future decades? A study of climatic variability in northern Europe [7] shows that variations in wind energy of up to 30% can be expected from one decade to another, see Fig. 5. In another study [2] it was found from an analysis of the expected power output for a 45-m high wind turbine over a 22-year period that the interannual variation in power corresponds to a mean relative standard deviation of approximately 13%.

For the proper assessment of the economics of wind power utilization, such variability must obviously be borne in mind. In comparison with other important factors such as rates of interest and prices of other fuels, the uncertainty in the wind resource is not large over the lifetime of a wind turbine of, say 20 years. Based

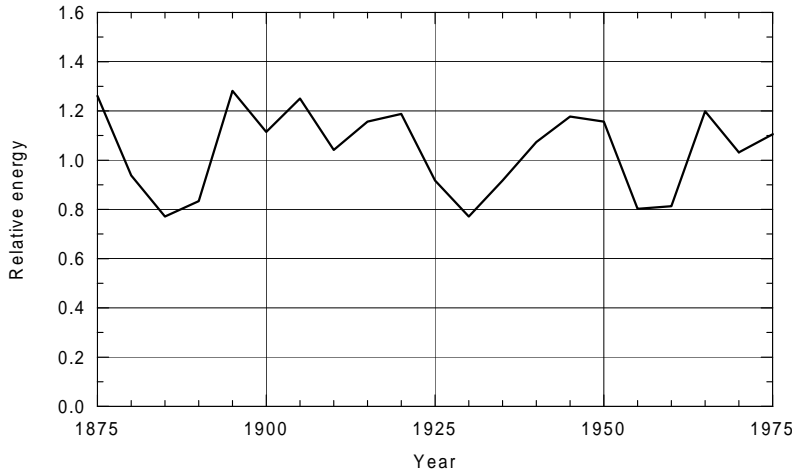


Figure 5. Mean energy in the wind for consecutive 5-year periods based on a time-series from Hesselø, Denmark, 1873-1982 [7].

on the studies cited above one can estimate the variation of the mean power from one 20-year period to the next to have a standard deviation of 10% or less. The possible effect of the increasing CO₂ content in the atmosphere might be a gradual change in the global climate. If this happens, both a change in the magnitudes of climate mean levels and climate fluctuations of the wind energy can be expected. However, as for now, no firm evidence of global change has been given.

4 WINDS IN THE ATMOSPHERIC BOUNDARY LAYER

The scientific discipline boundary layer meteorology has produced a wealth of knowledge, especially concerning the dynamics of the flow in the atmospheric boundary layer. Below, some of the aspects most important to wind power meteorology are described and the basic equations given.

4.1 Wind profiles and shear

The behaviour of the natural wind field over flat terrain of uniform roughness and a long upstream fetch is well known; both from a large number of field measurements and from theoretical treatments, and a description can be found in any textbook on turbulence [24].

The mean wind profile, i.e. measurements of wind speed as a function of height, averaged over periods of 10–60 minutes, is often described for engineering purposes by a power law approximation

$$\frac{U(z_1)}{U(z_2)} = \left(\frac{z_1}{z_2}\right)^p \quad (1)$$

where $U(z_1)$ and $U(z_2)$ are the wind speeds at heights z_1 and z_2 , respectively, and p is the power law exponent, with a typical value of 0.14. A serious problem with this approach is that p varies with height, surface roughness and stability, which means that Eq. (1) is of quite limited usefulness. A more realistic expression for the mean wind speed at height z , with much more general validity, can be

obtained from the so-called logarithmic wind profile with stability correction. This expression, which is well supported by theoretical considerations, is written

$$U(z) = \frac{u_*}{\kappa} \left(\ln \frac{z}{z_0} - \psi \right) \quad (2)$$

where u_* is the friction velocity, κ the von Kármán constant (≈ 0.4), z_0 the roughness length, and ψ a stability-dependent function, positive for unstable conditions and negative for stable conditions. The wind speed gradient is diminished in unstable conditions (heating of the surface, increased vertical mixing) and increased during stable conditions (cooling of the surface, suppressed vertical mixing), see Fig. 6(a).

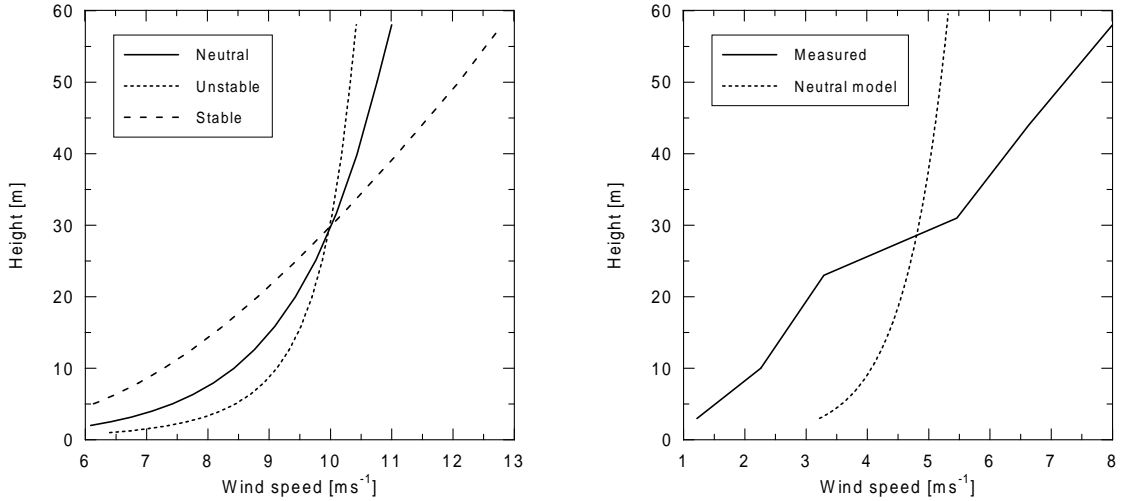


Figure 6. (a) Wind profiles for neutral, unstable and stable conditions according to Eq. (2). The profiles have been matched at 30 m, but represent the same roughness length. The mean wind speed gradient is very different for the same terrain and hub-height wind speed, but different stabilities. (b) Measured wind profile in very stable conditions with high wind shear (Nørrekær Enge wind farm, no-wake situation) [25, 26]. Neutral-model profile is for the same wind speed at 30 m and same roughness length.

In stable conditions, significant changes in wind direction with height are also observed. A wind turbine operating under such conditions experiences both a wind speed shear and a wind direction shear. An example of a large-shear case is given by the measured wind profile from the Nørrekær Enge II wind farm shown in Fig. 6(b) [25, 26]. The wind speed at hub height was quite moderate, but the very large shear across the rotor was comparable to the shear found with a hub-height speed of about 30 m s^{-1} in neutral conditions and a roughness length of 0.03 m. This situation gave rise to large loads at the rotation frequency. In fact, we first observed the anomalous loads, subsequently checked the data and then found the large wind shear situation.

As another example, typical values of mean wind shear across a 50-m rotor at 50-m hub height can for low wind speeds in stable conditions be of the same magnitude as the wind shear at very high wind speeds in neutral condition, i.e.:

Neutral	$z_0 = 0.03 \text{ m}$	$U_{\text{hub}} = 8 \text{ m s}^{-1}$	$U_{75} - U_{25} = 1.2 \text{ m s}^{-1}$
Stable	$z_0 = 0.03 \text{ m}$	$U_{\text{hub}} = 8 \text{ m s}^{-1}$	$U_{75} - U_{25} = 4.8 \text{ m s}^{-1}$
Neutral	$z_0 = 0.03 \text{ m}$	$U_{\text{hub}} = 32 \text{ m s}^{-1}$	$U_{75} - U_{25} = 4.8 \text{ m s}^{-1}$

The wind is generated by large-scale pressure differences and under certain simplifying circumstances a fictitious wind speed, the geostrophic wind, which is representative for the wind speed driving the boundary layer, can be calculated from the pressure field. Using information about surface roughness and stability, it is then possible to calculate the wind speed near the surface using the geostrophic drag law

$$G = \frac{u_*}{\kappa} \sqrt{\left[\ln \left(\frac{u_*}{fz_0} \right) - A \right]^2 + B^2} \quad (3)$$

where G is the geostrophic wind, f the Coriolis parameter, and A and B are dimensionless functions of stability (for neutral conditions, $A = 1.8$, $B = 4.5$). If the geostrophic wind is known, it is quite simple to calculate u_* for a given z_0 and use Eq. (2) for the calculation of the wind speed at a certain height. This is basically the double vertical extrapolation method described in the previous section.

In sloping terrain and over hills, certain layers of the flow accelerate, leading to different shapes of the wind profiles. The shear in local height ranges may then be much higher than that implied by Eq. (2), see Fig. 7(a). In-depth treatment of flow in changing terrain can be found in [27], and simple engineering approaches in [28] and [24].

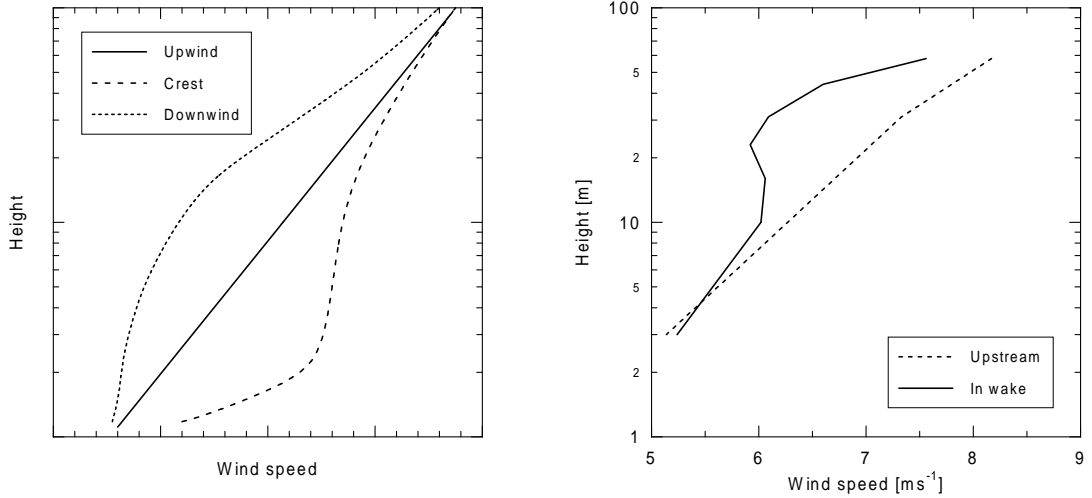


Figure 7. (a) Normalized wind profiles observed upwind, at the crest, and at the foot downwind of a two-dimensional ridge [27]. (b) Wind profiles upwind and 5.3 rotor diameters downwind of an operating wind turbine [26]. Seventeen time-series of 30-minute duration, with hub-height wind speeds in the range from 6 to 8 m s⁻¹ and near-neutral conditions, were selected for calculation of this average wind profile.

In the wake of an operating wind turbine, the mean flow speed decreases downstream of the rotor, giving rise to the formation of strong shear layers near the edges of the wake, especially near the top of the wake. Initially, the wake diameter is close to the rotor diameter, but as the flow moves away from the rotor, turbulent mixing gradually increases the wake diameter and decreases the velocity deficit. At a distance of about 10 rotor diameters downstream, the flow has almost recovered and the wind profile is close to the upstream profile. An example of the wind profile five rotor diameters downstream of a wind turbine is shown in Fig. 7(b), see also Fig. 10.

4.2 Turbulence and gusts

The turbulent variations of the wind speed are typically expressed in terms of the standard deviation, σ_u , of velocity fluctuations measured over 10 to 60 minutes, normalized by the friction velocity or by the wind speed. The variation in these ratios is caused by a large natural variability, but also to some extent because they are sensitive to the averaging time and the frequency response of the sensor used. In horizontally homogeneous terrain, the turbulence intensity, $I_u = \sigma_u/U$, is a function of height and roughness length in addition to stability, whereas σ_u/u_* , not too far from the ground, may be considered a function of stability only. A typical value for neutral conditions is $\sigma_u/u_* = 2.5$ for homogeneous flat terrain, often larger for inhomogeneous terrain, but with very large local variations.

The turbulence intensity is a widely used measure, and for neutral conditions with a logarithmic wind profile over flat terrain, we find $I_u \approx 1/\ln(z/z_0)$. Typical values of I_u for neutral conditions in different terrains are:

Flat open grassland: 13% Sea: 8% Complex terrain: 20% or more

Measurements from a number of sites were shown in [29]. The variations with stability can also be considerable, especially at low to moderate wind speeds, with smaller resulting turbulent intensities in stable conditions and larger values in unstable conditions; values of 25% are not unusual in flat open grassland for moderately unstable conditions. The variances are quite sensitive to the averaging time because much of the turbulent kinetic energy appears at quite low frequencies, in both unstable and particularly in stable conditions. In the latter case, the variance can be completely dominated by large-scale slow variations in wind speed and direction overlaid with very little turbulence [30].

In wakes we see increased turbulence levels together with decreased mean wind speeds, leading to significantly larger turbulence intensities than for the free flow [31, 32, 26, 33].

The turbulent velocity fluctuations can be described as a result of stochastic broadband processes. We see variations in velocity in a broad range of frequencies and scales, and numerous models have been used to describe the distribution of energy over different scales as a function of stability and height. These models can be subdivided into two ‘families’: the so-called Kaimal-spectra and their generalizations [34, 35, 36], providing good empirical descriptions of observed spectra in the atmosphere, and the von Kármán spectra, which may provide a good description of turbulence in tube-flows and wind tunnels, but are less realistic for atmospheric turbulence [37]. The popularity of the latter can mainly be attributed to the fact that they feature simple analytical expressions for the correlations. Examples of spectra in flat homogeneous terrain are shown in area-conserving representations in Fig. 8(a). Typical spectra, (at near neutral, and not too close to the ground) are dominated by broad maxima and falling off towards high frequencies as $f^{-5/3}$. The very low frequency behaviour is typically characterized by a large amount of variation and statistical uncertainty. Note the quite large differences in variances for different stabilities, with large variances in the unstable boundary layer and much smaller variances in the stable boundary layer.

The traditional way of relating length and time scales in turbulence is through the so-called Taylor ‘frozen turbulence’ approximation, i.e. the turbulence statistics can be regarded as a result of a frozen picture of turbulence advected past the observer by the mean wind, such that $\lambda = U/f$, where λ is a length scale and f the corresponding frequency observed in a fixed frame of reference. In the simple Kaimal formulation for neutral conditions, approached from stable conditions, spectra close to the ground have a dominating length scale of about 22 times the height above the ground. This is a fair approximation at low heights and moderate

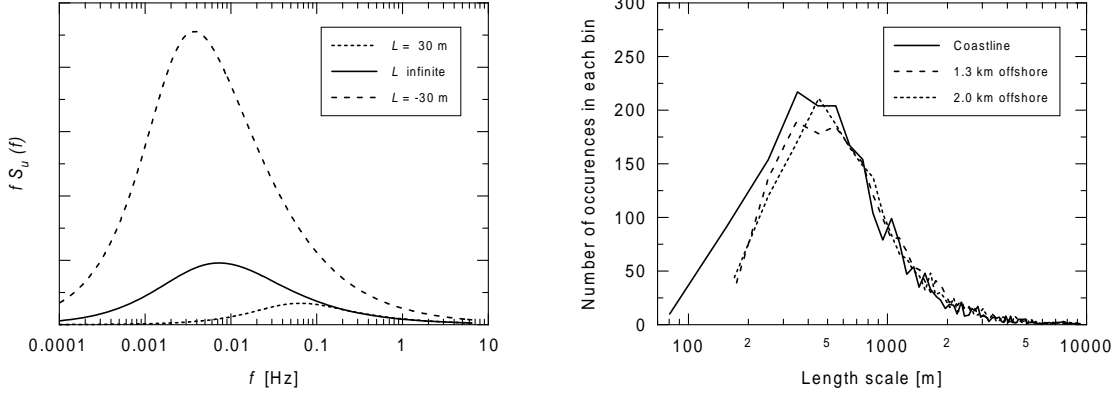


Figure 8. (a) Model spectra of the streamwise velocity component 50 m a.g.l. in flat terrain for neutral (L infinite), stable ($L = 30 \text{ m}$) and unstable ($L = -30 \text{ m}$) conditions, where L is the Monin-Obukhov length [34, 35, 36]. The areas under the curves are proportional to the variances. (b) Probability distribution of length scales from the Vindeby site at heights of 48 m. Length scales were derived by the ‘half variance’ method.

wind speeds, but above 30–40 m and for high wind speeds [38] the length scale approaches a constant value, typically 500–1500 m.

Terrain inhomogeneities may locally give rise to very large changes in the spectra. In flow over hills, the pressure field perturbations induced on the flow by the presence of the hill lead to an (almost) instantaneous redistribution of energy from the streamwise component of the wind to the vertical component by rapid distortion [39], see Fig. 9. In situations with changing roughness, the turbulence changes gradually downstream, first at small scales (high frequencies), and later also at larger scales. Because it can take considerable amounts of time (tens of minutes to hours) to change the large, energy-containing eddies, the turbulence of the flow ‘remembers’ the upstream conditions far downstream [40]. The general effect of inhomogeneous terrain is to increase turbulence, typically at length scales comparable in size to the characteristic terrain features [41]. In this way, the shape of the spectrum approaches that of the unstable spectrum in Fig. 8(a), where typical length scales of the energy-containing range are of the order of several kilometers.

Neutral conditions are very rare events, typically occurring only as transitions between stable and unstable conditions. However, near-neutral conditions occur also during overcast skies and moderate to high wind speeds. This variation in stability means that at a particular site, a wide range of dominating length scales are seen: from tens of meters to several kilometers, the distribution of which depends very much on the local stability climatology. The probability distribution of length scales at a coastal site is shown in Fig. 8(b). Here, the length scale was defined as the scale for which half of the variance of the streamwise component is distributed on larger scales and the other half on smaller scales. This length scale does not coincide exactly with the peak of the power spectrum – the difference being < 10% for a typical spectrum – but the length scale defined in this way is much easier to measure reliably. In Fig. 8(b), the most common length scale is 500–600 m, but the distribution is skewed (almost symmetric in the logarithmic representation) and the average length scale is about 1000 m. Length scale distributions are presented also for other heights in [33]; from 15 m and above these are very similar (for the 7-m level the scales were found to be significantly smaller) with a slight tendency towards smaller scales closer to land. Also, it has been observed at the offshore location, 2 km from the coast, that the scales are

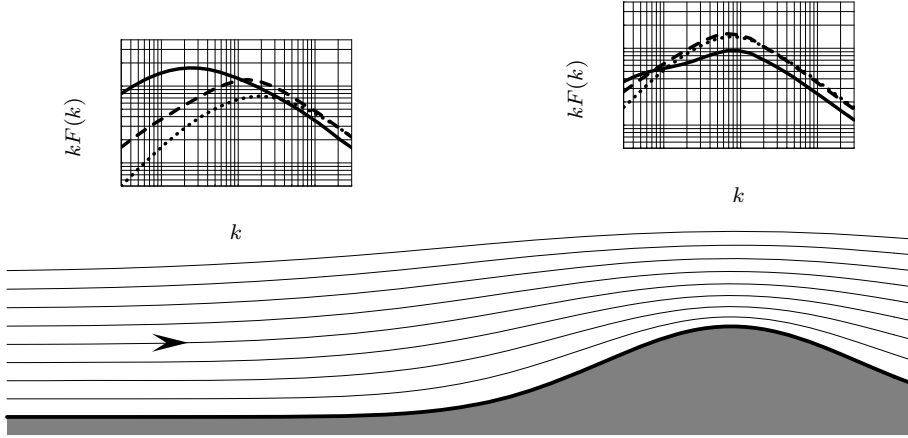


Figure 9. Wave-number spectra of the velocity components upstream and at the crest of a hill. Full line: streamwise, dashed line: lateral, dotted line: vertical. Note the redistribution of energy from the streamwise component to the vertical component by ‘rapid distortion’.

smaller for offshore flow and larger for onshore flow.

The spectral coherence, $\text{Coh}(f)$, is a useful measure of the normalized spectral distribution of spatial correlations. Note however that the integral of $\sqrt{\text{Coh}(f)}$ over all frequencies is different from the correlation. The spectral coherence is defined as

$$\text{Coh}(f) = \frac{Q_{12}^2(f) + Co_{12}^2(f)}{S_1(f)S_2(f)} \quad (4)$$

where Q_{12} is the quadrature spectrum, Co_{12} the cospectrum and S_1 and S_2 the power spectra measured at the physically separated positions 1 and 2. The coherence is an important quantity when translating Eulerian spectra into spectra in a rotating frame of reference, such as that ‘seen’ at a fixed position on a rotating wind turbine blade [42, 43]. It is quite difficult to measure coherences with sufficient statistical significance and consequently there is a lot of scatter in measured values. Traditionally, very simple exponential models have been used to describe the coherence functions [44], for coherences along the wind and perpendicular to the mean wind, in the lateral and in the vertical. The coherence for separations perpendicular to the mean wind in neutral conditions, is described well by the following model, even in wake situations [45]

$$\text{Coh}(f, \Delta s) = \exp\left(-\frac{a_i f \Delta s}{U}\right) \quad (5)$$

where Δs is the separation and a_i depend on the velocity component and the direction of separation (vertical or lateral). For the u -component $a_i = 12 + 11\Delta z/z_{\text{avg}}$ for vertical separation and $a_i = 12 + 11\Delta y/z$ for lateral separation – where Δz is the height difference, z_{avg} the average of the two heights, and Δy the lateral separation at the same height z . In the literature, several other models of varying degrees of sophistication can be found [46].

The coherences also depend on stability: the decay constant a_i increases significantly in stable conditions, and decreases slowly with increasing instability. In strongly stable conditions, the picture is somewhat blurred by the fact that the low-intensity, small-scale turbulent fluctuations are masked by the presence of slow, large-scale, highly coherent, two-dimensional structures. Except for minor differences in average stability (slightly more stable over the sea) there is no

reason to believe that the coherences should behave differently over the sea. In complex terrain, however, where we typically see excess turbulence at large scales, one might expect that, like for unstable conditions, the coherences will increase somewhat.

The presence of operating wind turbines in the flow have a significant impact on the flow properties close to the rotor (within 10 diameters), see [32, 26, 33, 47]:

- The wind speed is decreased inside the wake, giving rise to large shear at the top of the wake.
- Turbulence levels are increased inside the wake and, since the mean wind speed is decreased, there is a considerable increase in turbulence intensity.
- The length scale of turbulence is decreased inside the wake because the turbulence produced by the shear layers in the wake is created at length scales of the same magnitude as the cross-wind dimensions of the wake which are typically an order of magnitude smaller than the length scale of the turbulence in the free flow.
- Because of the wake-imposed length scale, turbulence length scales in the wake for the different components of wind speed approach each other.
- In general, second-order statistics is quite perturbed inside the wake and the usual boundary-layer approximations for variances etc. become quite different in the non-equilibrium turbulence in the wake.
- Spectral coherence in the wake seems to be well described by the usual models except for the near wake (distances $\leq 5D$), see [45].

Examples of changed mean and turbulence quantities are shown in Figs. 10 and 11.

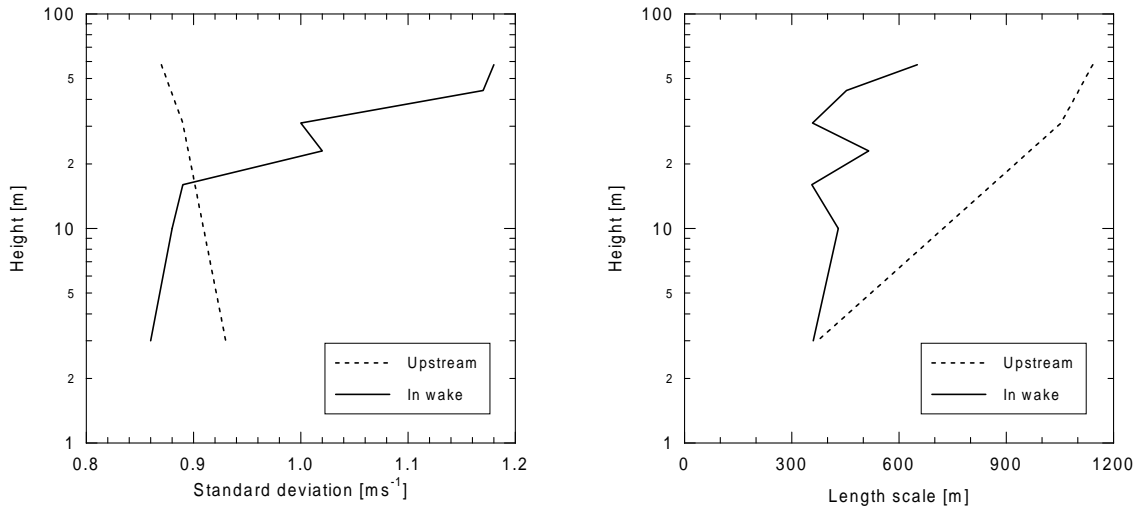


Figure 10. Profiles of (a) standard deviations of wind speed fluctuations and (b) length scales, upwind and 5.3 rotor diameters downwind of an operating wind turbine [26]. Hub height is 31 m and rotor diameter 28 m. Averages of 17 half-hour series with hub height speeds of 6–8 ms⁻¹ in near-neutral conditions were selected.

The turbulent velocity fluctuations, defined as the deviations of the instantaneous velocity from the average value (averaging time 5–60 minutes), are not the manifestations of a Gaussian process. Although probability distributions of wind

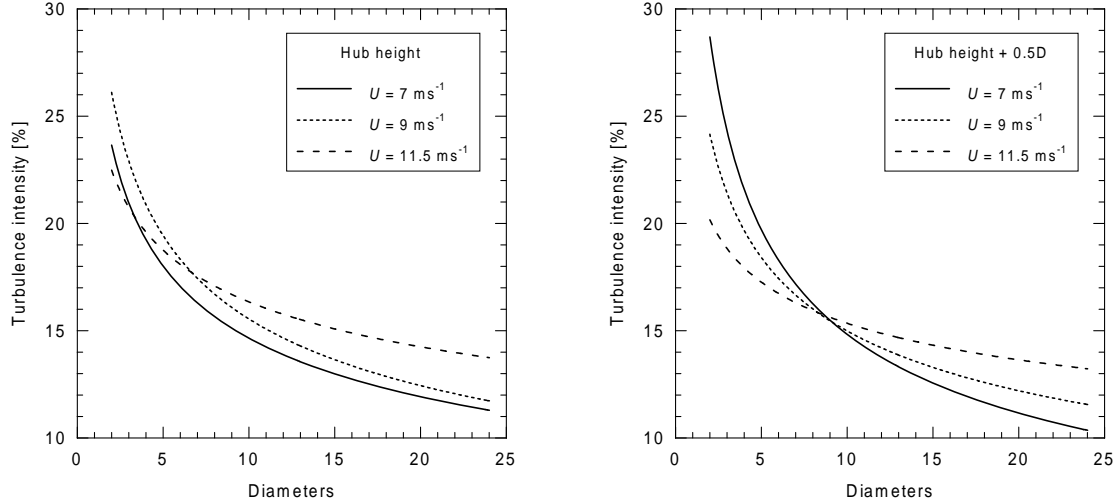


Figure 11. Downstream development of turbulence intensities at (a) hub height and (b) hub height + 0.5D, for three different wind speeds. The smooth curves were drawn through averaged data at 2D, 7.5D, 14.5D; undisturbed data correspond to 24 diameters downstream [45]. Hub height is 31 m and rotor diameter 28 m.

speed fluctuations to a good approximation follow a Normal distribution, accelerations are in general observed to have wider distributions ('longer tails') [48]. Despite these deviations and because of the lack of a better description, the gust, defined as the maximum wind speed during a measurement period of 5–60 minutes, is often calculated using a Gaussian process as an approximation [49, 50]. Using assumptions of stationarity, and that a wide-band process results in a joint-Gaussian description of u and du/dt , the expected gust value during time T , where we first have block-averaged data over time τ , is

$$\frac{U_{\max} - \bar{U}}{\sigma_u} = \sqrt{2 \ln \left[\frac{T}{2\pi} \frac{\sigma_{\dot{u}}(\tau)}{\sigma_u(\tau)} \right]} \quad (6)$$

where $\sigma_u(\tau)^2$ is the variance of wind speed fluctuations filtered with a lower cutoff at the frequency $1/T$ and block-averaged over time τ and $\sigma_{\dot{u}}(\tau)^2$ is the filtered variance of wind accelerations.

The results of such a calculation [51], using the Kaimal spectrum, are shown in Fig. 12(a), which also shows the results of simulated Gaussian turbulence [52] plotted as a function of the length scale (spectral peak) of the turbulence. Measured data from the Finnish Kopparnäs site are shown in Fig. 12(b) for different heights, plotted as a function of wind speed. These measurements are quite consistent with the model results, and show very little variation with height. The scatter around the curves is larger at low wind speeds and decreases towards higher speeds; typical standard deviations are 0.5 at 5 m s^{-1} and 0.4 at 15 m s^{-1} .

Another school of gust modelling takes its starting point in different characteristic shapes of gust events, that vary depending on the data set used. Some typical examples are described in [53].

For calculations of the mechanical loads on a wind turbine rotor, it is necessary to have detailed information about the spatial structure of the 3-D wind field. Many load models use the Veers-model [54], but in recent years the more efficient, realistic and flexible Mann-model has been developed [55].

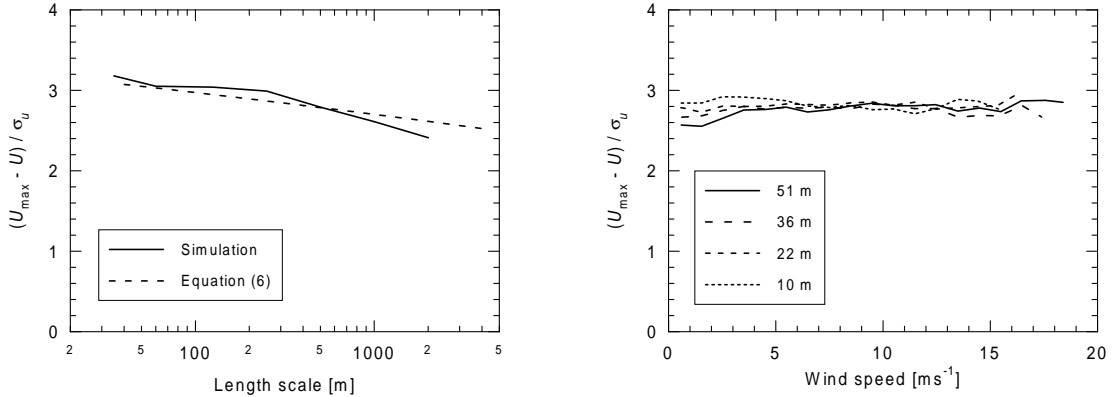


Figure 12. (a) Gust model calculations plotted as a function of length scale. Solid line is the result from a simulated time-series with 100 hours of simulated turbulence at each length scale. The dashed line was calculated using Kaimal spectra and Eq. (6). (b) Measured gust as a function of wind speed, using 10-minute time-series; approx. 1 second averaging time. Measurements at 10, 22, 36 and 51 m a.g.l. Typical standard deviations around mean values, 0.4–0.5, above 5 ms^{-1} .

4.3 Extreme winds and exceedance statistics

The proper design of a wind turbine for a specific wind climate must take into account the number of times, or the probability, that large loads and resulting large responses may occur over the lifetime of the turbine. As for other engineering applications, it is useful to use the return period T , which is the average time interval between excursions beyond a certain load. The largest loads are caused by the strong winds which occur in connection with severe weather phenomena. Most severe are undoubtedly tornadoes where it is claimed that wind speeds up to 100 m s^{-1} occur. A tornado is very localized with a horizontal extent of typically 500 m and a life time of tens of minutes. It is therefore almost impossible to estimate the probability that a specific location be hit by a tornado. However, it is well known that tornadoes are more prevalent in North America than in other places of the earth; about half of the world's tornadoes occur here and most of the other half occur in about 20 other countries. Very violent winds are also encountered in connection with the about 80 large-scale, severe storms – tropical cyclones, hurricanes and typhoons – that occur each year. The polar front in the northern latitudes is the cause of cyclones of large extent, thousand kilometers and with winds occasionally reaching the wind speeds of hurricanes and perhaps even tornadoes.

Good instrumental records are a necessary requirement for determining exceedance statistics. So are adequate statistical methods to determine the appropriate statistics and methods by which the statistics can be transformed from the location of the measurements to other locations. In engineering literature, extreme value statistics is often expressed as the average return period – typically 50 years – for a 10-min average wind speed of a certain (large) magnitude. Below, we illustrate a procedure for obtaining these statistics [56] by means of data from the Faroe Islands. The data series are all too short, but the analysis shows the principle as well as possible problems with the method. Data were measured on several islands in order to study the wind conditions at a range of typical topographical sites. The measurements during a severe storm are shown on Fig. 13(a) for the two islands of Nordradalsskard and Glyvursnes.

The first station is situated in a saddle point 267 m a.s.l. and is strongly affected by the orography, whereas the other station is considered not to be influenced by

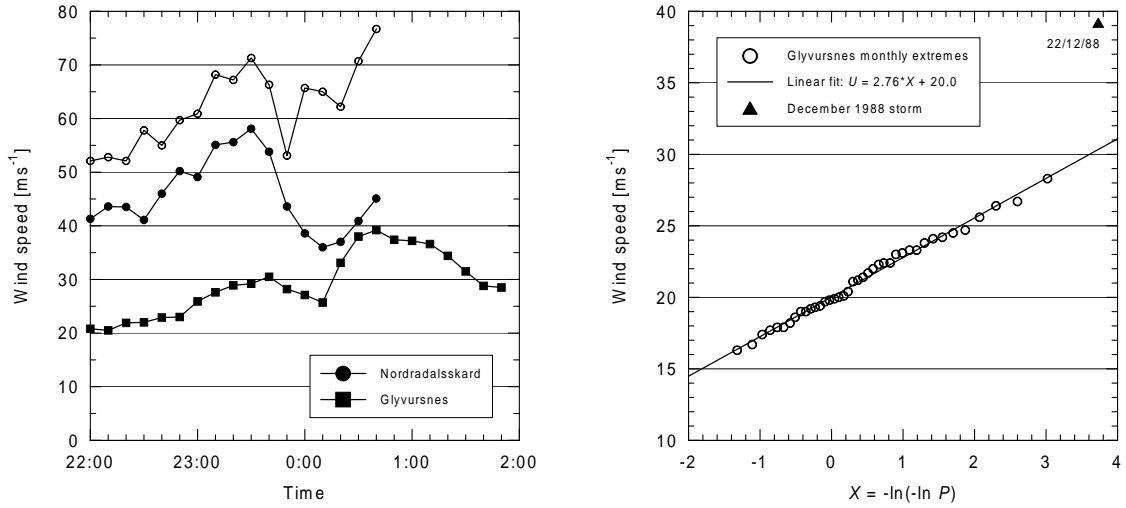


Figure 13. (a) Ten-minute averaged wind speeds at Glyvursnes and Nordradalsskard during a storm on the Faroe Islands, 21–22 December 1988. Two-second gust speeds (open circles) are also shown for the latter station. Measurements were taken 10 m a.g.l. The station most exposed to the storm ceased measuring a few minutes after 00:45 on the 22nd, when the lattice tower collapsed. (b) Monthly extreme wind speeds at Glyvursnes, irrespective of direction. P is given by $P = m/(N+1)$ where N is the size of the sample and m is an ordering number of the ranked events. The straight line is fitted disregarding the 21–22 December event.

the local topography. The largest 10-min mean wind speed at 10 m at the first station was 58.1 m s⁻¹ and the lattice tower carrying the instrumentation collapsed when the 2-sec gust value reached 76.7 m s⁻¹. The highest 10-min value at the second station was 39.2 m s⁻¹. The data series for the latter station covering 7 years is used for the extreme value analysis. First, the standard procedure [57] is followed by plotting ranked extreme events versus the double logarithm of their relevant probabilities and fitting a straight line. This gives the speed which on the average is exceeded once in the period T considered. The result is given in Fig. 13(b). The double exponential form of the accumulated probability function implies that for large (rare) events, the probability density function itself is nearly an exponential of the form $p(u) \approx \exp(-u)$. For such processes it can be shown that the average number of exceedances η per unit time of a certain speed u is proportional to $p(u)$ [50]. This can be used to extrapolate the above return period to another return period T . Thus, for one exceedance on the average, $T\eta$ is constant, i.e. $T_1 e^{-u_1} = T_2 e^{-u_2}$, or

$$u_2 = u_1 + \alpha \ln \frac{T_2}{T_1} \quad (7)$$

where α is the slope of the regression line in the ranking plot. Approximately the same results are obtained when other common statistical methods, e.g. selecting the events as individual storms, are used. The result is also rather insensitive to whether the analysis is carried out on the wind speed itself or the wind pressure. Finally, the estimated extreme value which is valid for conditions of 10 m above fairly open terrain, can be extrapolated to other topographical conditions and other heights at the island by applying the wind atlas method [58].

Figure 13(b) depicts a problem of the analysis: the storm event from Fig. 13(a) is completely off the regression line. If we use the parameters of this, calculated without the data from 22 October 1988, we obtain an average return period of approximately 300 years. However, this is an irrelevant and useless prediction.

The only conclusion we can draw is that this singular event must belong to a different phenomenon than the rest of the extreme value ensemble. We do not have a solution to such problems except to state that in order to get reliable extreme value statistics such as 50-year return periods, only long time-series of well measured data from a homogeneous statistical ensemble might suffice.

5 WIND CLIMATE DATA SOURCES

Different sources of wind data are available and can be employed for different purposes in wind energy studies – each type of data providing quite different levels of detail and accuracy. The overall distribution and magnitude of the wind resource on a global scale, the detailed mapping of the wind power potential on a national or regional scale, and the very detailed estimation of the actual power production by a wind turbine or wind farm, represent three very different scales within the broad range of applications in wind power meteorology.

5.1 Re-analysis projects

Useful sources of climatological data on a global scale are the re-analysis projects carried out by the National Centers for Environmental Prediction and National Center for Atmospheric Research, NCEP/NCAR [59], by the European Centre for Medium Range Weather Forecasting, ECMWF [60], or by NASA [61]. The projects objective is to produce homogeneous data sets covering a decade or more of weather analysis with the same data assimilation systems. This means that data from synoptic weather stations, radiosondes, pilot balloons, aircraft, ships, buoys, and satellites are collected, controlled, gridded and prepared for initialization of a global numerical weather prediction model.

The projects were initiated mainly to find low-frequency variabilities of the atmosphere. In routine weather analysis apparent (climatic) trends and jumps may appear when a new analysis scheme or forecast model is introduced. This unrealistic variability can be eliminated by using one state-of-the-art data assimilation system. In addition, data which were not available during operational weather forecasting can be included. The modern assimilation scheme plus the added input data should result in better analyses than the previous routine analysis.

The re-analysis data allow a broad overview of the global wind climate [62] and a first estimate in regions of poor observational coverage. A convenient property for the user of these data sets is their completeness. After the reanalysis there are no missing values in the data.

5.2 The synoptic network stations

For national and regional wind resource assessment, the routine observations carried out by the meteorological and other public services may be used, either as the primary data source or for verification purposes. In the Danish Wind Atlas [2], for example, the geostrophic wind climate was determined from long-term pressure measurements at about 55 synoptic stations in and around Denmark ($\approx 43\,000\text{ km}^2$). The geostrophic wind climate was then used to estimate the wind distributions at a given height over a specified terrain, by means of the geostrophic drag law [62]. The verification of the atlas was performed by estimating the wind climates of 12 specific sites in Denmark where long-term wind measurements had been carried out.

The European Wind Atlas [7], covering a land area of about 2.25 mio. km^2 , employed surface observations of wind speed and direction, measured over a 10-

year period, to determine the wind climate at about 190 European meteorological stations. In addition, 29 radiosonde stations were used to find the geostrophic wind climate at those locations. Using a set of physical models, the wind climates were subsequently referenced to a common set of standard topographical conditions, i.e. they were expressed as Weibull A - and k -parameters for five heights and twelve 30-degree sectors over four different values of surface roughness. Wind resource estimates for other sites can then be obtained invoking the same set of models to introduce the site-specific topography of these sites. The verification of the methodology was done in the same way, i.e. by intercomparison of the reference stations.

Most routine meteorological observations are presumably performed according to common (WMO) standards, but it should be borne in mind that wind energy was never the primary concern of these observational networks. Consequently, the selection and analysis of such data must be done very carefully. Evidently, the station data must cover the climatic area and time period of interest, but the anemometer should also be well exposed and an accurate history and description of anemometric conditions should be available. Time-series data should be preferred as the initial data source since this allows for detection of errors in the data which may be undetectable in data summaries. The data series and derived statistics should be inspected carefully to detect deficiencies in the data: abnormally high wind speeds (spikes), patterns in the data related to data transformation (e.g. from knots to m s^{-1}) or data transmission (truncation), representativity (daily/yearly), missing observations etc. The accuracy of the wind measurements should preferably also be evaluated, at least by visual inspection of the current anemometer setup.

5.3 On-site wind measurements

On-site wind measurements are often an important input to the prediction of the power production of a single wind turbine or wind farm (siting), or for establishing the power curve of a wind turbine. The accuracy of these measurements is crucial because the energy density and wind turbine power output are proportional to the cube of the mean wind speed. Furthermore, the instruments used must be robust and reliably accumulate data over extended periods of unattended operation.

Most on-site (and routine) wind measurements are carried out using simple mechanical devices like the traditional cup anemometer. The behaviour of these instruments is fairly well understood and the sources of error well known – but, alas, often neglected. Solid-state wind sensors (e.g. sonics) have until recently not been used extensively for wind energy purposes, mainly because of their high cost. Today, however, it has become feasible in large-scale projects – and certainly at wind turbine test centers – to deploy sonic anemometers. These have a number of advantages over mechanical anemometers and further provide measurements of turbulence, air temperature and atmospheric stability. However, they also introduce new sources of error which are less well known and the overall accuracy of sonic anemometry still needs to be investigated.

In general, the sources of error in anemometry include the effects of the tower, boom and other mounting arrangements, the anemometer design and its response to the turbulent characteristics of the flow and the calibration procedure. Evidently, proper maintenance of the anemometer is also important. In some cases, special problems arise due to icing of the sensor or deterioration of the mechanical parts of the anemometer at sites close to the sea. An overview of some important aspects of anemometry is given in Tab. 1.

The design considerations of cup anemometers are beyond the scope of this paper. A modern, sturdy, light-weight, fast-responding cup anemometer should

Table 1. Instrument characteristics and operational aspects that must be evaluated and taken into account in order to obtain accurate and reliable wind speed measurements using a cup or sonic anemometer. Evidently, the operational aspects are common to all anemometers.

Cup anemometer	Operational aspects	Sonic anemometer
• Anemometer design (ℓ_0)	• Calibration procedure	• Anemometer design
• u -bias $\propto (\sigma_u/U)^2$	• Siting of anemometer	• Array flow distortion
• v -bias $\propto (\sigma_v/U)^2$	• Tower, boom and clamps	• Transducer shadow effects
• w -bias $\propto (\sigma_w/U)^2$	• Environmental conditions	• Probe head geometry
• stress-bias $\propto \langle uw \rangle / U^2$	• Anemometer maintenance	• Transducer array characteristics

be used. The distance constant, ℓ_0 , i.e. the column of air corresponding to 63% recovery time for a step change in wind speed, should preferably be a few meters or less. An example of such an anemometer is the Risø-70 cup anemometer [63, 64].

The errors in cup anemometry caused by the turbulent nature of the wind have been discussed by many authors in the past; a thorough review of cup anemometer dynamics was recently given by Kristensen [64]. He discusses four types of biases: i) u -bias or ‘overspeeding’ causing too high measured wind speeds because the cup anemometer responds more quickly to an increase in the wind than to a decrease of the same magnitude; ii) v -bias or the so-called DP-error (data processing ‘error’) which accounts for the fact that the cup anemometer is not a vector instrument, but measures the mean of the total horizontal wind speed; iii) w -bias and iv) stress-bias which are equal to zero only if the anemometer has an ideal cosine response. The four turbulent biases are proportional to $(\sigma_u/U)^2$, $(\sigma_v/U)^2$, $(\sigma_w/U)^2$ and $\langle uw \rangle / U^2$, respectively [64]. The associated errors (ie with i, iii and iv) are in most cases of the order of 1% or less for a fast-responding anemometer mounted at a height of 10 m or more, but should be evaluated for the cup anemometer in question. The v -bias should be taken into account when comparing cup- and sonic-measured mean wind speeds.

Cup anemometers should be maintained and calibrated on a regular basis to ensure long-term accuracy in the wind speed measurements. It is usually recommended to perform the calibration in a wind tunnel, over the range of wind speeds of interest. However, since wind tunnel work is expensive and time-consuming – or a wind tunnel is simply not readily available – this is often not done. An alternative may be to intercompare cup anemometers in the atmosphere, i.e. to compare them to a reference instrument [65].

The tower or mast on which the anemometer is mounted interferes with the flow and therefore introduces errors in the measured wind speed and direction. For boom-mounted instruments this leads to a reduction in the wind speed measured downwind of the tower, as well as a smaller reduction in the wind speed measured on the upwind side. An example of the shadow effects from a lattice tower is shown in Fig. 14(a).

The width of the downwind sector angle in which the measurements are disturbed (typically $\pm 30\text{--}45^\circ$) is a function of the distance between the anemometer and the tower. However, no simple relationships exist because of the great variety of mast geometries. The distance should be at least 1.5 tower diameters [27], but preferably 3 or more. Since full 360° -coverage is often desirable in wind energy applications, two or more anemometers must then be operated at each level.

The boom and other mounting arrangements may also be the source of quite large errors in the measured mean wind speed, as shown by wind tunnel studies of the effect of various boom and clamp arrangements [66]. Long-term measurements using the same type of cup anemometer, Fig. 14(b), indicate that the effects may

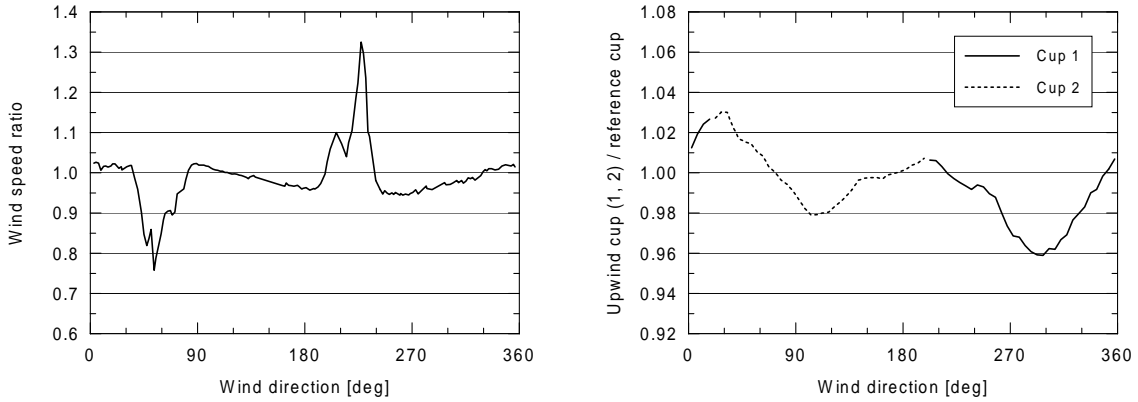


Figure 14. (a) Ratio of wind speeds measured by two cup anemometers versus wind direction. The cups are mounted on opposite sides of a triangular lattice tower with side length 1.2 m; the boom lengths are 2.5 m. (b) Ratio of wind speeds measured upwind of a lattice tower – by two boom-mounted cup anemometers – to an undisturbed reference speed versus wind direction. The distance between the cup rotors and the boom is 5.5 boom diameters.

be smaller in the atmosphere [65] than in the wind tunnel. However, both types of studies suggest that boom-mounted cup anemometers should generally be mounted on vertical extension poles with a distance between the rotor plane and the boom of at least about 12 boom diameters.

The adverse effects of the tower and mounting arrangements can (and should) be avoided by mounting one anemometer on a slender pole, about three or more tower diameters above the top of the tower – without lightning conductors or antennas. This is particularly important if only one anemometer position is available.

The improper siting of a well-calibrated and properly mounted anemometer can easily render the measurements useless. Hence, if wind measurements are not made at the exact point of interest, e.g. at hub height at the location of a wind turbine, some effort should go into siting of the anemometer. The effects of topography on a number of possible sites may be estimated using numerical models, e.g. the WASP models [7, 9]. In order to minimize subsequent modelling uncertainties, the anemometer site should resemble as closely as possible the sites that are to be investigated (predicted), i.e. with respect to elevation, exposure, ruggedness, land use, and height above ground.

The sonic anemometer measures the wind speed from the flight times, t_1 and t_2 , of ultrasonic sound pulses traveling in opposite directions across a fixed sound path [27]. It has no moving parts and therefore none of the response problems associated with cup anemometers. By the same token, it presumably requires very little maintenance. The wind speed measured along a sound path, S_ℓ , is a function of the path length and the two travel times only: $S_\ell = (\ell/2)(1/t_1 - 1/t_2)$; i.e. independent of atmospheric conditions like pressure, air temperature, humidity, etc.

Lack of ease-of-operation, long-term instability and high cost have been major obstacles to the application of sonic anemometers in wind energy studies. However, several sonic systems are now fairly easy to operate and can provide data over extended periods of time. Furthermore, a number of systems have become available at a cost comparable to the total cost of a cup anemometer, wind vane and temperature sensor (including booms, clamps, cabling, radiation screen etc.).

The major concern, inherent in sonic anemometry, is the fact that the probe head itself distorts the flow – the effect of which can only be evaluated in detail by

a comprehensive wind tunnel investigation [67, 68, 69, 70]. The transducer shadow effect is a particularly simple case of flow distortion and a well-known source of error in sonics with horizontal sound paths [27]. Less well known are the errors associated with inaccuracies in probe head geometry [70] and the temperature sensitivity of the sound transducers [70]. Finally, specific details in the design of a given probe head may give rise to wind speed-dependent errors [68]. Wind tunnel investigations and atmospheric sonic intercomparisons carried out at NCAR and Risø [70] suggest that the accuracy and reliability of common off-the-shelf sonic systems are approaching those of a fast-responding, calibrated cup anemometer. However, the cup anemometer should still be employed for accurate determinations of the mean wind speed. For measurements of the three-dimensional structure of atmospheric turbulence the sonic anemometer seems to be the instrument of choice.

6 TOPOGRAPHY

The wind close to the earth's surface is strongly influenced by the nature of the terrain surface, the detailed description of which is called *topography*. The interaction between the wind and the surface takes places on a broad range of length scales, and much effort in boundary-layer meteorology has been devoted to the separation of this range of scales into a number of characteristic domains which can be systematically described, parameterized and/or modelled. For the purpose of wind power meteorology, which is primarily concerned with the wind flow from 10 to 200 meters above the ground, the effects of the topography can be divided into three typical categories [7]:

Roughness The collective effect of the terrain surface and its roughness elements, leading to an overall retardation of the wind near the ground, is referred to as the roughness of the terrain. The point of interest must be 'far away' from the individual roughness elements, and the height usually much larger than the height of these.

Obstacles Close to an obstacle, such as a building or shelter belt, the wind is strongly influenced by the presence of the obstacle which may reduce the wind speed considerably. To be of any consequence, the point of interest must be 'close' to the individual obstacle, and the height comparable to the height of the obstacle.

Orography When the typical scale of the terrain features becomes much larger than the height of the point of interest, they act as orographic elements to the wind. Near the summit or the crest of hills, cliffs, ridges and escarpments, the wind will accelerate while near the foot and in valleys it will decelerate.

This division of the topography – simple as it may seem – has proven extremely useful in wind power meteorology [7] and it is invoked routinely [9] to describe the complexity of the 'real world'. Some terrain characteristics and concepts used for the description and analysis of topography are introduced below.

6.1 Surface roughness

The roughness of a terrain surface can be parameterized by a single length scale, the roughness length z_0 , the influence of which on the wind speed profile was given by the logarithmic wind profile and the geostrophic drag law. Since the roughness of an area is determined by the size and distribution of the roughness elements it contains – including vegetation, built-up areas, and soil and water surfaces

- the roughness length is not constant, but changes with foliation, growth of vegetation, snow cover, sea state and so on. This should be taken into account in any climatological analysis.

Land-use information, from which the roughness may be derived, can be extracted from topographical maps, aerial photographs, satellite imagery, data bases on surface cover, or by visual inspection of the site(s) of interest. In any case, the information is usually a snap-shot only of the land-use. The site-specific roughness lengths and changes of roughness can be described in a *roughness rose*, corresponding to the up-wind conditions in a number of sectors. However, it is much more convenient to record the information in a *roughness map* and let the analysis model extract the specific information needed [9]. Roughness maps can readily be derived from most land-use data bases, in which case an automatic procedure may be set up. This facilitates wind resource assessment over large areas vastly.

Coastal land- and seascapes, in demand for wind power utilization because of the generally high wind resource, are characterized by large roughness changes at the coast-line. Recently, offshore sites have also attracted considerable attention. Prediction of the wind climate in these environments, where relatively few observations exist, requires detailed knowledge about the roughness of water surfaces.

Offshore conditions present a situation where the flow in many respects differs from that over land. Some of the more significant differences are (greatly simplified):

- The roughness length is very small for moderate wind speeds leading to:
 - Small vertical wind gradients
 - Small turbulence intensities
- The roughness length is not constant, but varies with:
 - Wind speed (z_0 increases rapidly with increasing speed)
 - Upstream distance to land (higher roughness close to land)
 - Water depth
- Stability conditions are also different from inland conditions because of the high heat capacity of the sea:
 - The average stratification is slightly stable in mid-latitudes away from warm or cold sea currents.
 - The daily cycle in the stability variation over land is replaced by a seasonal cycle with stable conditions in spring-summer and unstable conditions in fall-winter.
 - The roughness change from land to sea is large and the effect of upstream roughnesses can extend far offshore. The height of the internal boundary layers developing after a roughness change grows much more slowly in stable than in a neutral or unstable conditions, and the general turbulence level is also lower which further decreases the growth rate.

Wind turbine wakes extend their effect further downstream, and their relative impact is larger offshore than onshore because of the low turbulence levels and the stability.

In near-coastal areas, which initially are the most interesting ones for wind energy purposes, the situation becomes further complicated:

- The sea surface roughness varies because of changes in the wave field near the coast.
- The large roughness change between land and sea is ‘felt’ by the flow a significant distance offshore.

- Coastal orography will influence the flow at sea both for off- and onshore wind.
- Differential heating of land and sea surfaces will superimpose secondary flows (sea and land breezes) on the synoptic flow pattern.
- In areas with very cold water like the Baltic Sea, the phenomenon known as low-level jets may bias the local climate towards higher wind speeds than those derived from the usual geostrophic approximations [71].

Some of these problems are dealt with in detail in a study of the Baltic Sea wind resources [72].

A widely used expression for the roughness length of the open, deep sea far from land is the so-called ‘Charnock’ expression [73]:

$$z_0 = A \frac{u_*^2}{g} \quad (8)$$

where g is the acceleration due to gravity. The value of the constant A is usually quoted as 0.01–0.04, where the lowest value is for open sea and the highest value is for near-coastal conditions, see Fig. 15. Recent research [74] has shown that the ‘constant’ A actually varies by a factor of more than 10 as a function of ‘wave age’, i.e. young, developing waves extract much energy from the wind and, consequently, the roughness is high; old waves extract much less energy and their roughness is therefore significantly lower.

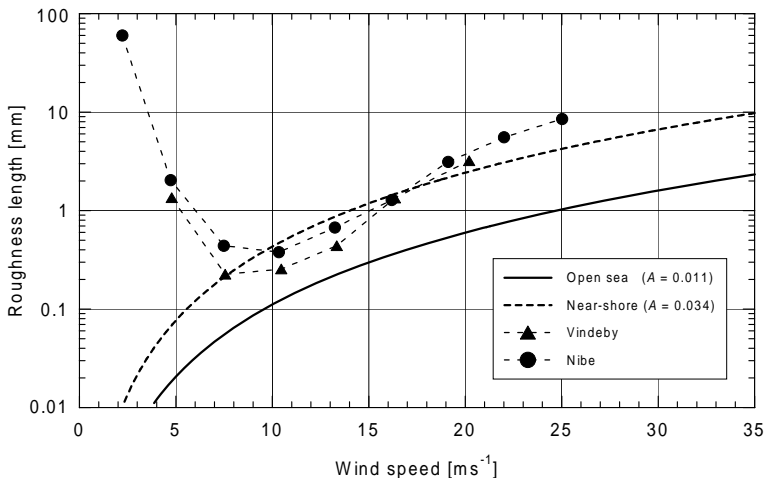


Figure 15. Calculated and measured offshore roughness lengths as functions of wind speed. Curves for two values of the Charnock constant using Eq. (8) are shown. They represent open sea and near-shore conditions, respectively. The measured roughness lengths were derived from data at a coastal site, Nibe, and a near-coastal site, Vindeby. Wind directions with upstream fetches over water of 7–15 km were used in both cases. Roughness lengths were derived from near-neutral data using $I_u = 1/\ln(z/z_0)$. Twelve years of measurements from Nibe [75] were used, and one year from Vindeby [76, 33]. The high, measured values at low wind speeds are partly due to instabilities and stability effects.

At very high wind speeds, the sea surface roughness approaches that of a smooth land surface. This should of course be taken into account when considering extreme loads, where the turbulence added to the extreme wind speeds will have the same magnitude over land and sea.

6.2 Obstacles

The second local effect which must be taken into account is the sheltering of e.g. the anemometer by near-by obstacles, such as buildings. Obstacles may be extracted from detailed maps, but it is usually advisable to visit the site as well. The site visit, or analysis of aerial photography, is also necessary for determining the height and porosity of obstacles. The information needed for shelter modelling is basically the dimensions, position, and porosity of each obstacle. If a site is severely sheltered, the wakes may further be characterized by wake moment coefficients [77].

6.3 Terrain orography

The term *orography* refers to the description of the height variations of the terrain, referenced to a common datum such as the mean sea level. The orography is described in most topographical maps by the height contour lines of the terrain surface. Height contours can also be specified in digital form as a *vector map*, which contains the (x, y) -coordinates and elevation of the contour lines. Some flow models, e.g. the BZ-model of WASP, employ digital maps directly. Other models require a Cartesian grid of terrain spot heights, a so-called digital terrain model (DTM) or *raster map*. Accurate raster maps can readily be derived from detailed vector maps, whereas the transformation of raster maps to vector maps results in some loss of information, depending on the actual grid cell size of the DTM. For the purpose of wind energy applications, we here divide the different landscapes into three simple classes: flat, hilly and mountainous, see Fig. 16. In *flat* terrain and lowland regions far from mountains, the orographic effects are negligible and the roughness of the terrain is the all important characteristic for the wind flow; examples of this were given above.

By *hilly* terrain we mean terrain which is sufficiently gentle to ensure mostly attached flow, corresponding to landscapes where the slopes are less steep than about 0.3. Typical horizontal dimensions of the hills are a few kilometers or less. This type of landscape is generally within the operational envelopes of present-day linearized flow models and several bench-mark data sets exist for the testing of flow models in such terrain [78]. As the terrain gets steeper and more complex, and the typical horizontal dimensions of the hills increase to several kilometers, the large scale orographic features may induce strong modifications of the entire boundary layer. Linearized models may still give accurate results locally, but horizontal extrapolation of the wind climate becomes increasingly difficult.

In *mountainous* terrain a significant fraction of the slopes are steeper than about 0.3 and flow separation occurs. In addition, the entire boundary layer is strongly influenced by the terrain. In general, the flow cannot be adequately be modelled using simple linearized models; non-linear, numerical models or measurements must be used.

The somewhat indeterminate term ‘complex terrain’ is often used in connection with the orographic characteristics of a landscape; applied primarily for hilly and mountainous terrain consisting of a ‘complex’ mixture of several hills or mountains. However, no widely accepted measure of terrain complexity exists at present.

One objective measure of the steepness or ruggedness of the terrain around a site is the so-called *ruggedness index* or RIX [79], defined as the percentage fraction of the terrain steeper than some critical slope, say 0.3 [80]. This index was proposed [79] as a coarse measure of the extent of flow separation and thereby the extent to which the terrain violates the requirements of linearized flow models. Based on the limited experience available, the landscapes in Fig. 16 may be characterized by the following RIX values: flat and hilly 0% (upper panel), more complex (lower

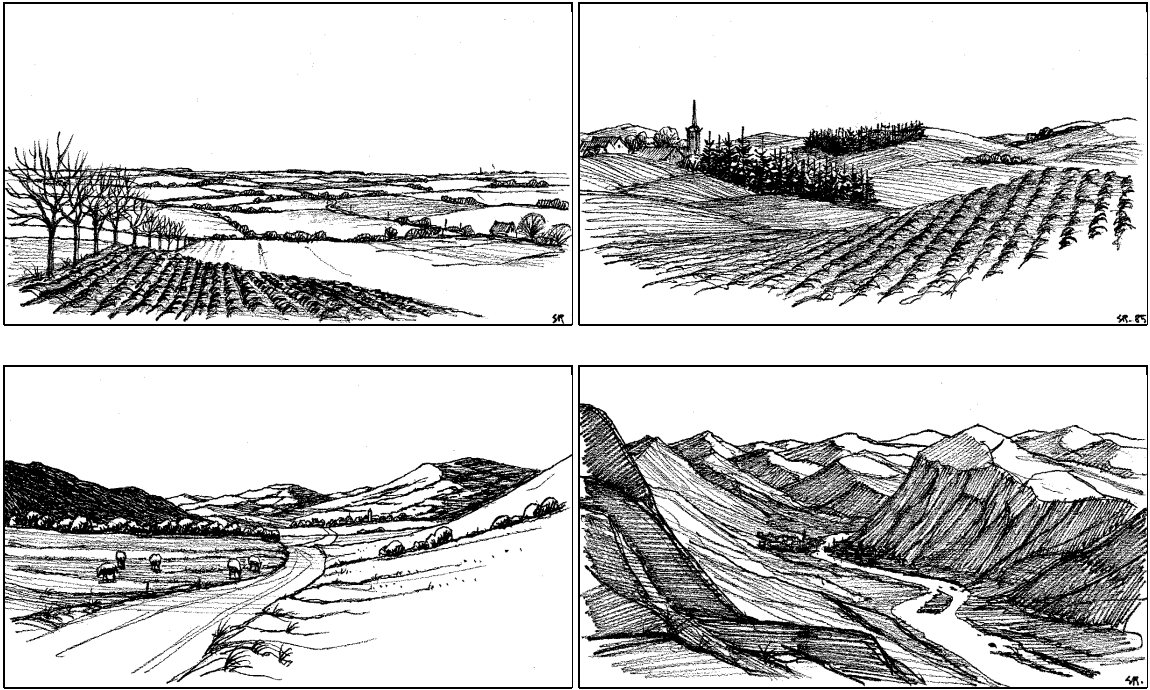


Figure 16. Different landscape types [7]: flat (upper left) and hilly (upper right) terrain is generally within the performance limits of linearized flow models. As the terrain gets steeper and more complex (lower left) the modelling uncertainties become larger and present-day engineering models must be applied with utmost care. The flow in mountains cut by deep valleys (lower right) may be investigated using more advanced flow models and/or by measurements. (S. Rasmussen del.)

left) about 10% or less, mountainous (lower right) from about 10 to 50% or more.

The ruggedness index has also been used to develop an orographic *performance indicator* for WASP-predictions in complex terrain [79, 81] – where the indicator is defined as the difference in the percentage fractions (ΔRIX) between the predicted and the reference site. This indicator may provide the sign and approximate magnitude of the prediction error for situations where one or both of the sites are situated in terrain *well outside* the recommended operational envelope, see Fig. 17.

The systematic trend in Fig. 17(a) indicates a strong influence of flow separation on the WASP wind speed prediction error [79]. If the reference and predicted sites are equally rugged, i.e. $|\Delta\text{RIX}|$ small, the prediction errors are relatively small. If the reference site is rugged and the predicted site less rugged or flat, the overall prediction is underestimated with a significant negative error. Conversely, if the reference site is flat or less rugged than a rugged predicted site, the overall prediction is overestimated with a significant positive error.

Figure 17(b) shows the same data, but arranged according to the ruggedness index of the most rugged of the two sites. This figure indicates that accurate wind speed predictions may be obtained even in mountainous terrain, provided that the difference in ruggedness indices between the reference and predicted site is small. This is obviously the case for the self-prediction at any category of site, but may also occur for neighboring sites with similar orographical settings and orientation. This represents an important application involving the prediction of wind speeds and power production at adjacent sites along a steep ridge in a wind farm.

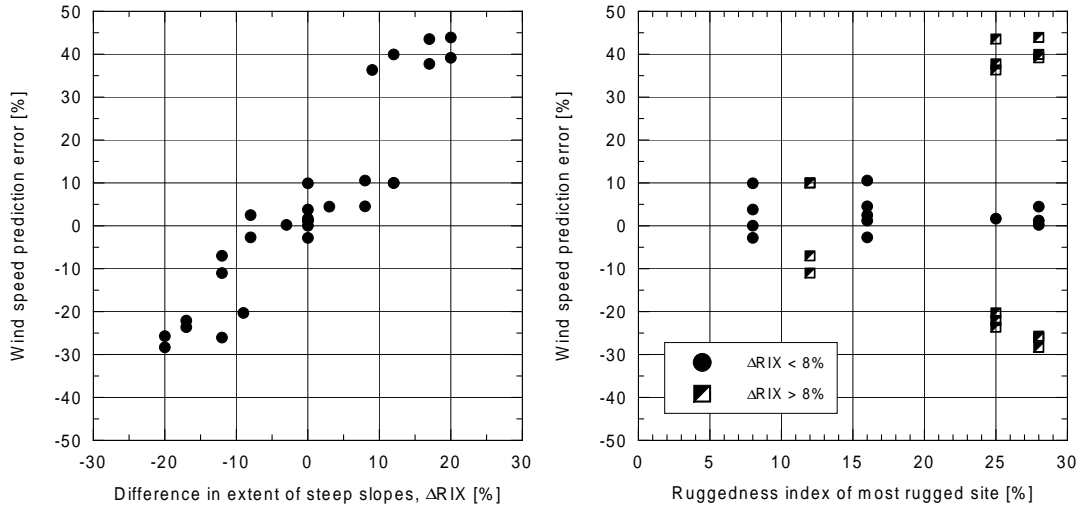


Figure 17. (a) WA^sP wind speed prediction error versus the difference in extent of steep slopes (RIX values) between the predicted and the reference site [79, 81]. Data from five Portuguese and two French sites are shown. (b) WA^sP wind speed prediction error versus the extent of steep slopes (RIX value) of the most rugged of the predictor (reference) and predicted site [81]. Same data as (a).

7 METEOROLOGICAL MODELS

As the wind is a very local characteristic, influenced by the surrounding hills and changes of roughness, one needs methods of interpolation for wind measurements. In addition, measurements are costly to carry out, and it takes a long time to obtain climatological estimates. Therefore, models are needed for the interpolation between measurements and for the prediction of the wind climate. By prediction we do not mean the prediction of weather or climatic variability, but the calculation of the wind climate at a specific site without measurements at that site.

A meteorological model is in this context any model which allows one to calculate wind fields in the atmosphere. Models range from global, numerical weather prediction models (NWP) to models for flow over small hills or roughness changes. The latter contain no humidity processes, and often not even a temperature equation. Nevertheless, many of these are very useful for the calculation of the local wind field. Global NWP models have too coarse a resolution for detailed mapping of the wind resource. Therefore, the emphasis here is on mesoscale and smaller scale models.

7.1 Input to models

A full NWP model needs input data on the wind, temperature, and humidity fields in the atmosphere and also in the soil. However, for wind energy applications one often wants to have only climatological wind values without the need for exact daily forecasts. In this case, the following data at the model boundaries are the most important:

- The orography and roughness of the terrain. The roughness length can be derived from a specification of the land-use and vegetation coverage.
- The climatology of the external forcing which, for most mesoscale and microscale models, is larger-scale pressure gradients, or background flow fields, as well as solar insolation.

Initial conditions are quite similar and initial wind and temperature fields have to be specified. Often, they are derived from larger-scale fields which reflect the larger-scale climatology. One important point for simulations with daily cycles of insolation is the specification of the initial time and date of the simulation. This is clearly the case for weather prediction. However, for climatological studies it is not obvious which date to choose and no objective method is known at present. – Observations enter as both boundary and initial conditions through the climatology.

The main large-scale parameters influencing the surface wind in mid-latitudes are the geostrophic wind and the stratification of the atmosphere. Temperature differences between land and sea can also be important, especially in coastal regions. The main surface parameters are surface elevation and roughness length, and soil or sea surface temperature.

7.2 Classifications of models

The following list contains different classifications of models. Loosely, one could say that for most of the criteria complexity increases from left to right.

dynamics: kinematic (mass-consistent), hydrostatic, non-hydrostatic

advection: linear, non-linear

time domain: diagnostic, prognostic

spatial scale: microscale, mesoscale, synoptic

stratification: neutral, non-neutral

friction: frictionless, turbulent closure

formulation: analytical, spectral, grid point

type: flow model, wind climate model

In reality, the classification is more complex. As an example, WASP is a linear model; however, the interaction of its stability model and the roughness change model is non-linear. Also, its hill-flow model assumes neutral stratification, but the mean wind field is for non-neutral stratification.

7.3 Limitations of and requirements to models

In the following we discuss briefly some limitations and assumptions of the different models which influence their application.

Mass-consistent models contain no dynamic equations, they only require the flow field to be divergence free. Therefore, they require many observations in order to model the flow field correctly [82, 83]. They should not be used if only one observation point is available.

In hydrostatic models the equation for vertical momentum is substituted by hydrostatic equilibrium. They should only be used to model the regional wind climate, i.e. resolved scales greater than ~ 10 km. The hydrostatic assumption will lead to wrong phases of the speed-up above small mountains and hills. Instead of being at the summit as observed, the maximum speed-up is predicted at the lee-side of the hill.

Linear models calculate deviations, u' , from a base or reference state, U . Theoretically, they should work only for small perturbations, say $u'/U < 0.2$. However, in practice u'/U up to about 0.5 still works well. They can not calculate detached flow, which occur in steep terrain with slopes greater than approximately 0.3 [80].

However, they are very fast and easy to use and this makes them very attractive. Most linear models are diagnostic models. Non-linear models require more computing resources.

The scale of the model influences which forces must be included in the model. In a terrain where the length scale of the variations is less than approximately 10 km, Coriolis forces are not important for calculating perturbations from the mean flow. However, non-hydrostatic accelerations are important on small hills. This is just the reverse for synoptic-scale flows, where Coriolis effects cannot be neglected, but the hydrostatic approximation works well.

Friction is important for flow near the surface. However, models with very simple or essentially no surface friction describe atmospheric flows surprisingly well, because the direct effects of friction are confined to a shallow layer near the surface [84]. Also, the description of the deformation of turbulence in flow over hills by rapid-distortion theory is frictionless.

Most linear, spectral models use Fast Fourier Transforms to solve for variations in the horizontal directions, assuming periodic domains. Atmospheric mesoscale models are grid point models and they should have open boundaries. WASP employs polar coordinates. Consequently, it is not periodic, though it is a spectral model.

The distinction between flow models and wind climate models concerns mainly the ease of use of the models for wind power applications. WASP is mainly a wind climate model. It is very easy to use for wind power applications, where the focus is on a small number of specific sites, but not very convenient for the calculation of flow fields. Other meteorological models more easily calculate the individual flow fields. However, it is also more complicated to determine wind climatologies from these individual calculations. Wind climate models must contain a flow model. In addition, they often do the data assimilation in order to establish the climatology.

The choice between different models depends on the application in question, the available computing and human resources and the available input data. A good model can never make up for bad input data. Therefore, it is important to find accurate and efficient descriptions of the climatology of the input data. For WASP, this description is given by the Weibull parameters in different direction sectors.

7.4 Combined meso/micro-scale modelling

An efficient method of predicting the surface wind climate is to combine a mesoscale model and a microscale model. The mesoscale model simulates the regional wind climate like flow over and around mountain ranges and in large valleys. The local model calculates the speed-up and sheltering by hills, local obstacles, and local roughness conditions. Such a procedure is illustrated in Fig. 18, where the Karlsruhe Atmospheric Mesoscale Model, KAMM [85, 86], is combined with the microscale model WASP [7, 9]. KAMM calculates the mesoscale wind field using as input a description of the synoptic scale climatology, as well as orography and roughness maps. The climatology of the simulated wind fields and the local orography and roughnesses are subsequently used by WASP to predict the local wind climate.

The statistical-dynamical approach of regionalization of large-scale climatology [87] is used to calculate the regional surface wind climate with KAMM. It is assumed that the regional surface layer climate is determined uniquely by a few parameters of the larger synoptic scale, plus the parameters of the surface. This parameter space is decomposed into several representative situations and numerical simulations of these are performed with the mesoscale model. The mesoscale climatology is finally calculated from the results of the simulations together with the frequency of the typical situations.

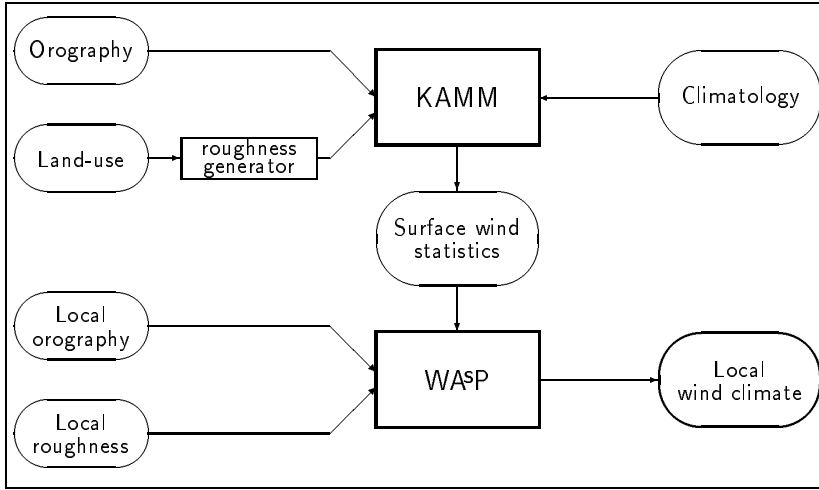


Figure 18. Schematic presentation of the KAMM/WASP approach to calculate the local wind climate.

The simulations are processed in a similar way as the measurements, i.e. the simulated winds are transformed to a number of standard roughnesses and standard heights using the geostrophic drag law. Then, Weibull distributions are fitted to the transformed wind speeds to construct the so-called wind atlas data sets which, in turn, constitute the input for WASP. The wind atlas files represent the generalized regional wind climate and are established for each grid point of KAMM. The local wind climate can now be determined using WASP together with the wind atlas data from the nearest grid point.

This approach has been used to model the wind climate of Ireland [88, 89]. Figure 19 shows the simulated wind energy density 50 m above a flat surface with roughness length $z_0 = 3$ cm calculated by the KAMM model.

The data shown in Fig. 19 can be used to predict the yearly power production of a wind turbine using WASP. In Fig. 20, such production estimates are compared to power production estimates obtained directly from measurements at 18 sites in Ireland – where the vertical extrapolation of these measurements to hub height was carried out using WASP. The agreement is good, except for the very low productions, where the simplified modelling of stability effects leads to large differences.

7.5 Short-term prediction

The wind is highly variable and difficult to predict (forecast). This causes problems for the electrical utility dispatchers since they have to schedule the operation of conventional power plants not knowing the production from the wind farms. If the penetration level (fraction of the total power delivered by wind turbines) is low this constitutes a minor problem and wind energy can be considered a negative consumer. In areas with high penetration levels, however, addressing the problem in this way would cause an unnecessary use of fossil fuels, leading to economic losses and pollution of the atmosphere. As an example of an area with high penetration, the Jutlandic and the Funen part of Denmark may have up to 40% of the electricity produced by wind farms at certain times.

To avoid this waste of fossil fuel, the wind resource has to be predicted. This can be done using numerical weather prediction (NWP) models of the general atmospheric circulation. These models predict the overall motion of the atmosphere, e.g. low-pressure systems. To predict the winds in a specific wind farm, it is nec-

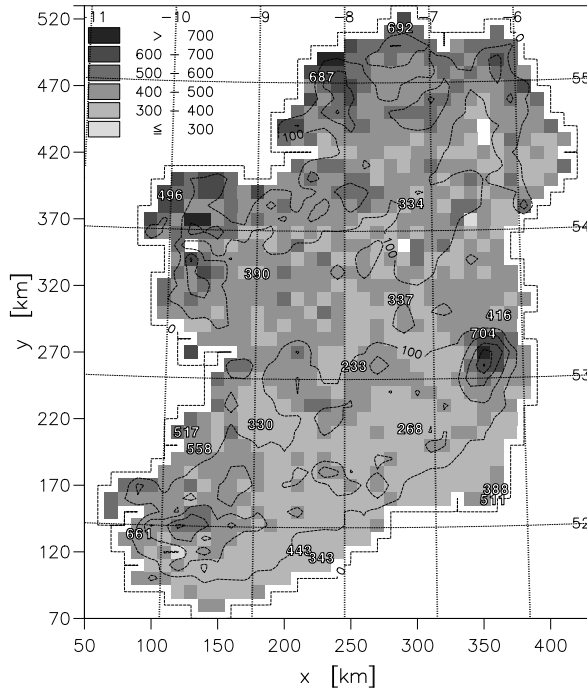


Figure 19. Wind power density in Wm^{-2} at a height of 50 m and roughness length $z_0 = 3 \text{ cm}$ over Ireland calculated by KAMM. Values from a wind atlas analysis by WASP are shown at the positions of 18 stations.

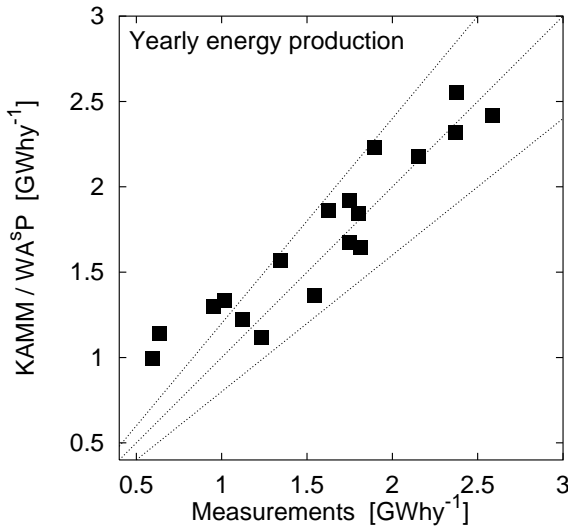


Figure 20. Comparison at 18 sites of the predicted yearly power production in GWh^{-1} of a Vestas V42 600-kW wind turbine (y-axis) and the power production estimated by vertical extrapolation of wind measurements (x-axis).

essary to transform the overall wind field to the surface, taking the local effects in the wind farm into account. Local effects are typically associated with orography, roughness, near-by obstacles, and the presence of other wind turbines.

Risø has developed a model which is based on the idea outlined above [90, 91]; a diagram detailing the model is shown in Fig. 21. The model is based on NWP-predictions from the High Resolution Limited Area Model (HIRLAM) of the Dan-

ish Meteorological Institute [92], the local topographical corrections are calculated by WASP [9], and the wind farm wake effects and productions are calculated using the PARK code [93]. The output and performance of the model are described briefly below.

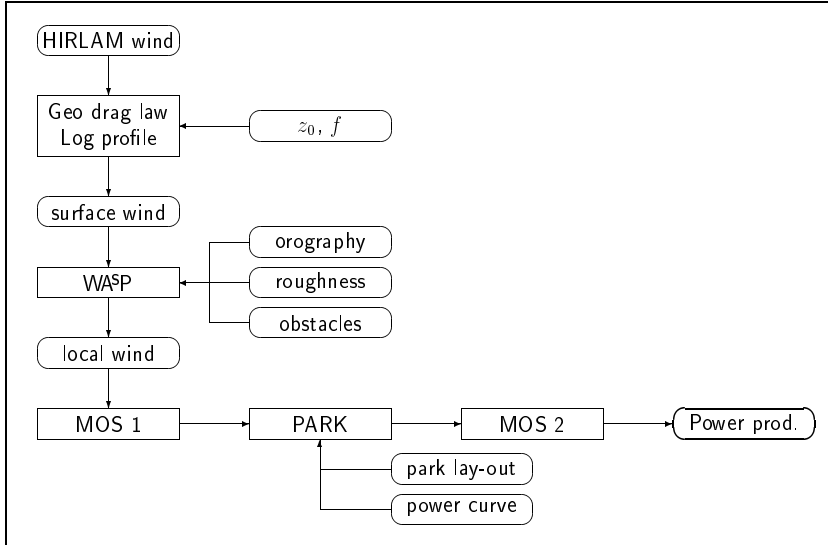


Figure 21. Flow chart of the prediction model. MOS is short for Model Output Statistics.

For ease of electronic transfer, the model predictions are provided as HTML-files, i.e. the file format used on the World Wide Web (WWW). The advantage of this is, that if the utility is large, it can run the model at its own premises and view the HTML-files locally. If a number of smaller utilities have joined together, they can view the pages via the Internet. The files contain the 12 forecasts (from +3 to +36 hours ahead) for the total production (if applicable) and for each wind farm. It is envisaged that the utility is provided with software (i.e. a Web-browser) to display the forecasts. This type of output makes the prediction system *platform independent*.

Since the beginning of 1997 the model has been running on-line, predicting the production of a large number of wind farms in Denmark, Great Britain and Greece. The HIRLAM predictions are sent via the Internet to Risø. At Risø a system is set up that runs the power prediction model every time a new forecast arrives. The output from this model is HTML files which are automatically put on the Internet as WWW-pages. The HIRLAM model run is available about two and four hours after its verify (initialization) time, depending on the geographical location of the wind farm. The time in transit between DMI and Risø (or the utility) is insignificant, and the power prediction model runs in less than a minute for all the wind farms. Since the HIRLAM model is run twice a day, the Web-pages are also updated twice a day with a new 36-hour forecast. The latest development is that the HIRLAM prediction horizon has been extended to 48 hours.

To give an example of the general performance of the model, results obtained from a previous study are given below. A total of 17 wind farms were modelled for an entire year, from February 1995 to January 1996 [94]. The performance for the one-year period of one of these wind farms (Kynby, Zealand, DK) is shown in Fig. 22.

It can be seen from this, that in the first four hours the so-called persistence model (stating that what is measured now, is the prediction at any time in the

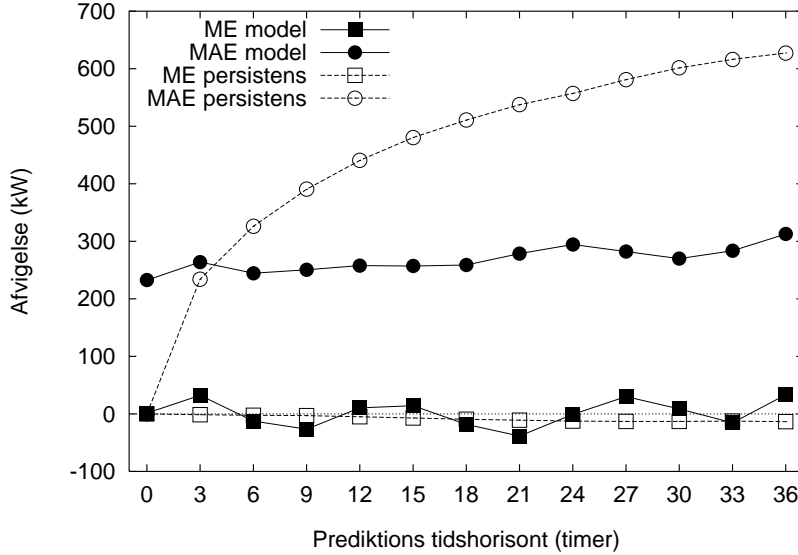


Figure 22. The performance of the Risø model compared to the persistence model for the Kyndby wind farm, using a full year's worth of data. The rated power of the wind farm is 3.78 MW, i.e. the error never exceeds 10% of the rated power. The forecast length in hours is along the x-axis. ME is the mean error (squares) and MAE the mean absolute error (circles).

future) performs better than the developed model; after this time the model is superior. It can also be seen that the mean absolute error (i.e. the scatter) seems to increase only very slowly with look-ahead time. A detailed analysis of the model performance and the error is given in [91].

As an example of the detailed performance of the model, the first real fall storm in Europe in 1997 has been predicted. To that end, measurements from the 118-m mast at Risø National Laboratory were used. The measurements, along with the model predictions, are plotted in Fig. 23. It appears that the development of the storm was predicted extremely well and also well in advance: at no point in time are the predictions more than 3 m s^{-1} away from the measurements and for most of the duration of the storm, they are well below this limit. The storm was predicted about 30 hours in advance, leaving utilities ample time to schedule the conventional power plants. In the potentially critical high-wind area, close to the cut-out wind speed of most turbines, the model predicts the wind speed accurately. Wind speeds below 5 m s^{-1} do not contribute to wind turbine power production and wind speeds between 15 m s^{-1} and 25 m s^{-1} provides maximum power output. Therefore, the prediction of wind speeds in the interval from 5 m s^{-1} to 15 m s^{-1} is particularly important for estimating the power production at any given time accurately. The model predictions are also close to the measured data in this wind speed range. The excellence of these predictions is entirely due to the prediction skills of the HIRLAM model.

8 AREAS OF FURTHER RESEARCH

It is our hope that this overview article on wind power meteorology will initiate a number of articles on central topics by authors well versed in this discipline. It is also foreseen that contributions will come from basic disciplines such as me-

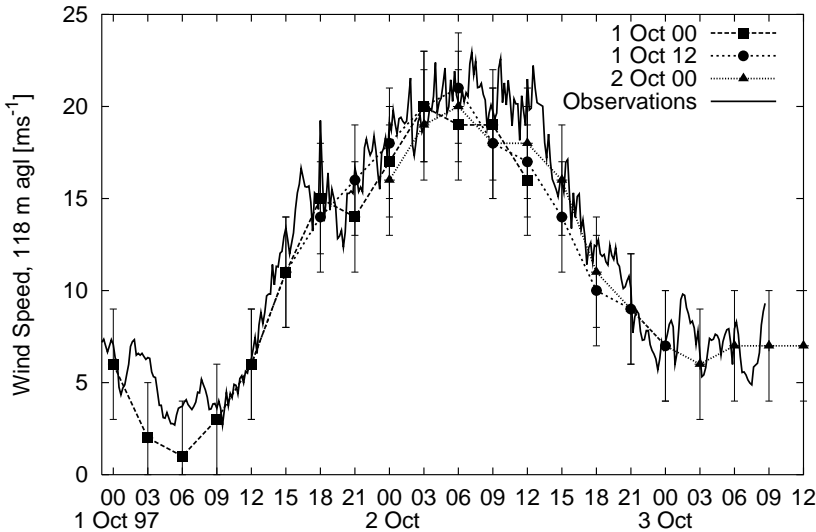


Figure 23. Predictions and measurements for the Risø mast. Three consecutive Risø-model predictions are shown, the first from 1 October 1997 at 00 UTC, the next at 12 UTC and the third from 2 October 1997 at 00 UTC. For each of the predictions, the expected error is also shown by vertical error bars. The measurements are plotted every 10 min.

teorology, climatology, geography, fluid dynamics, time-series analysis, stochastic processes etc. Overall, it is essential that the contributions add to the general knowledge on the utilization of wind energy. Well undertaken and well described research will help the wind energy community to accelerate progress by avoiding wasting time and effort.

The following list of areas of further research reflects our view and therefore can not be complete. A more general view can be found in [95] where the European wind energy research community has put forward a ‘road map’ for future R&D in wind energy.

Weather and wind climate:

- Systematic methods for the description of the ‘large-scale’ climate.
- The variability of the wind climate, temporally and spatially, i.e. how much does the expected energy output vary from year to year in different parts of the world.
- Extreme winds as a function of location, locally (influence by local topographic features) and globally.

Winds in the atmospheric boundary layer:

- Realistic models for the turbulence in real terrain. How can the results from simplified models be applied to real-life conditions, and how large variations are to be expected around ‘standard conditions’?
- Wind turbine wake models are used routinely for modelling the mean flow, but some of the pertinent questions remain only partly answered or unanswered: What are the merits and drawbacks of the different models? How do we model turbulence realistically in the wake?
- Disturbed wind and turbulence fields close to obstacles, forests, cliffs etc., modelling and measurements, and their effects on wind turbines.

Wind climate data sources:

- Optimal use of the large databases – such as the NCAR/NCEP or ECMWF re-analysis data, the COADS data [96], the CORINE (Coordination of Information on the Environment) land use data, the world-wide orographic and land use data – for regional wind resource assessment and siting of wind farms.
- Systematic acquisition, description, analysis and presentation of wind data from entire regions, interesting localities with high wind energy potential and tall towers (the wind turbines are growing out of the surface layer).

Topography:

- The use of satellite observations and ‘ground truth’ measurements to determine surface roughness, its seasonal variation and ‘climatological’ value.
- The use of satellite data in general for wind energy, especially wind in offshore areas.
- Realistic models for propagation of noise from wind farms in all types of terrain, but especially mountainous terrain.
- Objective measures of terrain ruggedness and complexity. Topographical analysis.
- Complete wind farm studies including: site calibration, wind flow modelling, and comparison of predicted and actual production.

Meteorological models:

- Objective measures of the applicability and quality of flow models, in particular in complex and mountainous terrain. How much data are needed for flow model verification, and what are proper performance indicators for wind climate prediction.
- The use of meso-scale models for wind resource assessment: data for initial and boundary conditions, presentation and use of resulting statistics, and parameterizations.
- Further work in short-term prediction.

Acknowledgements

Much of the work by Risø National Laboratory on wind energy in general and wind energy resources in particular have – since 1981 – been supported by the Commission of the European Union, Directorate-General for Science, Research and Development. The Danish Energy Agency of the Ministry of the Environment and Energy has supported many of the national wind energy and wind power meteorology projects through the EFP-program. The offshore measurements at the Vindeby site were further sponsored by the Office of Naval Research, the Danish Technical Research Council, and the Danish utility ELKRAFT. The wind data from the Faroe Islands are presented by courtesy of S. P. Heinesen, Landsverkfrødingurin (Office of Public Works), Faroe Islands. Field data on the boom and clamp effects affecting cup anemometers were kindly provided by G. Jensen, Risø. The KAMM modelling was carried out with permission from F. Fiedler and G. Adrian, University of Karlsruhe. HPF was sponsored by the European Commission through the program “Training and Mobility of Researchers”.

Last, but definitely not least, we would like to thank Dr. L. Kristensen, Risø, for his thorough review of and comments to an early draft of the paper.

References

- [1] D. L. Elliott, C. G. Holladay, W. R. Barchet, H. P. Foote and W. F. Sandusky, *Wind Energy Resource Atlas of the United States*, Solar Energy Research Institute, Golden, Colorado 1986.
- [2] E. L. Petersen, I. Troen, S. Frandsen and K. Hedegaard, *Windatlas for Denmark. A rational method for wind energy siting*, Risø-R-428, Risø National Laboratory, Roskilde, Denmark 1981.
- [3] R. M. Traci, G. T. Phillips, P. C. Patnaik and B. E. Freeman, *Development of a Wind Energy Methodology*, U.S. Dept. Energy Rep. RLO/2440-11, 1977.
- [4] T. R. Hiester and W. T. Pennell, *The Siting Handbook for Large Wind Energy Systems*, Windbooks, New York 1981.
- [5] P. A. Taylor and R. J. Lee, 'Simple Guide Lines for Estimating Wind Speed Variations due to Small Scale Topographic Features', *Climatol. Bull.*, **18**(2), 3–32 (1984).
- [6] P. Vermeulen, A. Curvers, B. van den Haspel, J. Leene, D. van der Velden, J. Wieringa and A. van Wijk, 'Further Development of a Dutch handbook for Wind Energy Production Estimates' *Proceedings of the European Wind Energy Assoc. Conf. and Exhibition*, Rome, Italy, **1**, 1986, pp. 219–223.
- [7] Troen, I. and E. L. Petersen, *European Wind Atlas*, Risø National Laboratory, Roskilde, Denmark 1989.
- [8] A. S. Monin and A. M. Yaglom, *Statistical Hydrodynamics*, MIT Press, Cambridge 1975.
- [9] N. G. Mortensen, L. Landberg, I. Troen and E. L. Petersen, *Wind Atlas Analysis and Application Program (WASP)*. Vol. 2: User's Guide, Risø-I-666(v.2)(EN), Risø National Laboratory, Roskilde, Denmark 1993.
- [10] J. A. Børresen, *Wind atlas for the North Sea and the Norwegian Sea*, Norwegian University Press and Norwegian Meteorological Institute, Oslo 1987.
- [11] J. Højstrup, *Wind Atlas for Jordan*, Risø National Laboratory, Roskilde, Denmark 1989.
- [12] S. J. Dear, M. J. Bell and T. J. Lyons, *Western Australian Wind Atlas and Supplement – Atlas Program*, Report no 64, Minerals and Energy Research Institute of Western Australia, Perth 1990.
- [13] S. Kunz and R. Hugentobler, *Meteo Norm, Wind Leitfaden für den Windenergieplaner*, Bundesamt für Energiewirtschaft, Bern 1990.
- [14] R. Hammouche, *Atlas vent de l'Algérie*, Office National de la Météorologie, Alger 1991.
- [15] B. Tammelin, *Finnish Wind Atlas*, Finnish Meteorological Institute, Helsinki 1991.
- [16] R. Krieg, *Vindatlas för Sverige*, SMHI Energi-anläggning, Norrköping 1992.
- [17] S. Traup and B. Kruse, *Winddaten für Windenergienutzer*, Selbstverlag des Deutschen Wetterdienstes, Offenbach am Main 1996.
- [18] N.G. Mortensen and U. Said Said, *Wind Atlas for the Gulf of Suez. Measurements and modelling 1991–95*, Risø National Laboratory, Roskilde, Denmark 1996.
- [19] H.-T. Mengelkamp and A. Raabe, 'Wind Power Estimation over Complex Terrain', *Proceedings of the 1993 European Community Wind Energy Conference*, Travemünde, Germany, 1993, pp. 587–590.
- [20] E. L. Petersen, N. G. Mortensen, L. Landberg. 'Measurements and modelling in complex terrain', *Proceedings of the 1996 European Union Wind Energy Conference*, Göteborg, Sweden, 20–24 May, 1996, pp. 580–583.
- [21] H. H. Lamb, *Climate: Present, Past and Future, Vol. 1: Fundamentals and Climate Now*, Methuen & Co Ltd, London 1972.

- [22] H. E. Landsberg and C. C. Wallen (eds.), *World Survey of Climatology*, Vol 1–15, Elsevier, Amsterdam, 1969–85.
- [23] World Meteorological Organization, *Meteorological Aspects of the Utilization of Wind as an Energy Source*, WMO Technical Note 175, World Meteorological Organization, Geneva, Switzerland 1981.
- [24] H. A. Panofsky and J. A. Dutton, *Atmospheric Turbulence. Models and Methods for Engineering Applications*, John Wiley & Sons, New York 1984.
- [25] C. J. Christensen, M. S. Courtney and J. Højstrup, ‘Turbulence and turbine dynamics in a windfarm’, *The Potential of Windfarms, Conference Proceedings*, Herning, Denmark 1992, D4 1–7.
- [26] J. Højstrup, M. S. Courtney, C. J. Christensen and P. Sanderhoff, *Full scale measurements in Wind-Turbine arrays, Nørrekær Enge II*, CEC/JOULE, Risø-I-684, 1993.
- [27] J. C. Kaimal and J. J. Finnigan, *Atmospheric boundary layer flows. Their structure and measurement*, Oxford University Press, New York, 1994.
- [28] E. Simiu and H. Scanlan, *Wind Effects on Structures. Fundamentals and Applications to Design*, John Wiley & Sons, New York 1996.
- [29] J. Højstrup, ‘The turbulent wind field in various terrain types and in windfarms’, *Proceedings from IEA-symposium on Wind Conditions for Wind Turbine Design*, Hamburg, June 1994, pp. 3–15. Proceedings available from Dept. of Fluid Mechanics, Technical University of Denmark.
- [30] S. E. Larsen, H. R. Olesen and J. Højstrup, ‘Parameterization of the low frequency part of spectra of horizontal velocity components in the stable surface boundary layer’, *Turbulence and Diffusion in Stable Environments*, ed. J. C. R. Hunt, Clarendon Press, Oxford 1985, pp. 181–204.
- [31] J. Højstrup, ‘Probability structure of turbulence in a windfarm’, *Proceedings from 20th Meeting of Experts – Wind Characteristics of Relevance for Wind Turbine Design*, ed. B. M. Pedersen and R. Windheim, Kernforschungsanlage Jülich, 1991, pp. 15–19.
- [32] J. Højstrup and P. Nørgård, *Tændpibe windfarm measurements 1988*, Risø-M-2894, Risø National Laboratory , Roskilde, Denmark 1990.
- [33] S. Frandsen (Ed.), L. Chacon, A. Crespo, P. Enevoldsen, R. Gomez-Elvira, J. Hernandez, J. Højstrup, F. Manuel, K. Thomsen, and P. Sørensen., *Measurements on and Modelling of Offshore Wind Farms*, Risø-R-903, Risø National Laboratory, Roskilde, Denmark 1996.
- [34] J. C. Kaimal, J. C. Wyngaard, Y. Izumi and O. R. Coté, ‘Spectral Characteristics of surface layer turbulence’, *Q. J. R. Meteorol. Soc.*, **98**, 563–589 (1972).
- [35] J. Højstrup, ‘Velocity spectra in the unstable boundary layer’, *J. Atmos. Sci.*, **39**, 2239–2248 (1982).
- [36] H. R. Olesen, S. E. Larsen and J. Højstrup, ‘Modelling velocity spectra in the lower part of the planetary boundary layer’, *Boundary-Layer Meteorol.*, **29**, 285–312 (1984).
- [37] J. Højstrup ‘Velocity spectra’, *Proceedings from IEA-symposium on Wind Conditions for Wind Turbine Design*, Risø, Denmark, April 1993, pp. 51–57. Proceedings available from Research Centre Jülich, Germany.
- [38] J. Højstrup, S. E. Larsen and P. H. Madsen, ‘Power spectra of horizontal wind components in the neutral atmospheric surface boundary layer’, *AMS 9th Symposium on Turbulence and Diffusion*, Roskilde, Denmark 1990, pp. 305–308.
- [39] A. A. Townsend, *The structure of turbulent shear flows*, 2nd ed., Cambridge University Press, 1976.
- [40] J. Højstrup, ‘A simple model for the adjustment of velocity spectra in unstable conditions downstream of an abrupt change in roughness and heat flux’,

- Boundary-Layer Meteorol.*, **21**, 341–356 (1981).
- [41] H. A. Panofsky, D. Larko, R. Lipschutz, G. Stone, E. F. Bradley, A. J. Bowen and J. Højstrup, ‘Spectra of velocity components over complex terrain’, *Q. J. R. Meteorol. Soc.*, **108**, 215–230 (1982).
- [42] L. Kristensen and S. Frandsen, ‘Model for power spectra measured from the moving frame of reference of the blade of a wind turbine’, *J. Wind Eng. Ind. Aerodyn.*, **10**, 249–262 (1982).
- [43] L. Kristensen, ‘Power spectra and cross-spectra as seen from the moving blade of a wind turbine’, *J. Wind Eng. Ind. Aerodyn.*, **12**, 245–250 (1983).
- [44] A. G. Davenport, ‘The spectrum of horizontal gustiness near the ground in high winds’, *Q. J. R. Meteorol. Soc.*, **87**, 194–211 (1961).
- [45] J. Højstrup, ‘Spectral coherence in wind turbine wakes’, *J. Wind. Eng. Ind. Aerodyn.*, **80**, 137–146 (1999).
- [46] L. Kristensen and N. O. Jensen, ‘Lateral coherence in isotropic turbulence and in the natural wind’, *Boundary-Layer Meteorol.*, **17**, 353–373 (1979).
- [47] G. C. Larsen, J. Højstrup and Helge Aagaard Madsen, ‘Wind fields in wakes’, *Proceedings of the 1996 European Union Wind Energy Conference*, Göteborg, Sweden, 20–24 May, 1996, pp. 764–768.
- [48] J. A. Dutton and J. Højstrup, ‘A probabilistic model of turbulent velocity fluctuations’, *Proceedings from Wind Characteristics and Wind Energy Siting Conference*, Oregon 1979, pp. 59–67.
- [49] L. Kristensen, M. Casanova, M. S. Courtney and I. Troen, ‘In search of a gust definition’, *Boundary-Layer Meteorol.*, **55**, 91–107 (1991).
- [50] N. O. Jensen, J. Mann and L. Kristensen, ‘Aspects of the natural wind of relevance to large bridges’, *Proceedings of the first International Symposium on Aerodynamics of Large Bridges*, ed. A. Larsen, Copenhagen, Denmark, February 1992, pp. 25–32.
- [51] J. Højstrup and B. Tammelin, ‘Wind resources in complex coastal terrain’, *Proceedings of the 1996 European Union Wind Energy Conference*, Göteborg, Sweden, 20–24 May, 1996, pp. 544–547.
- [52] J. Højstrup, ‘A statistical data screening procedure’, *Meas. Sci. Technol.*, **4**, 153–157 (1993).
- [53] F. J. Verheij, J. W. Cleijne and J. A. Leene, ‘Gust modelling for wind loading’, *J. Wind. Eng. Ind. Aerodyn.*, **42**, 947–958 (1992).
- [54] P. S. Veers, *Three dimensional wind simulation*, Sandia National Laboratories, SAND88-0152, 1988.
- [55] J. Mann, ‘The spatial structure of neutral atmospheric surface-layer turbulence’ *J. Fluid Mech.*, **273**, 141–168 (1994).
- [56] E. L. Petersen and N.O. Jensen, ‘Storms: statistics, predictability and effects’, *Natural Risk and Civil Protection*, ed. T. Horlick-Jones, Aniello Amendola and R. Casale, Chapman & Hall, London, 147–177, 1995.
- [57] N. J. Cook, *The Designer’s Guide to Wind Loading on Building Structures*, Butterworth, London 1985.
- [58] J. Abild and B. Nielsen, *Extreme Values of Wind Speeds in Denmark*, Risø-M-2842, Risø National Laboratory, Roskilde, Denmark 1991.
- [59] E. Kalnay, M. Kanamitsu, R. Kistler, W. Collins, D. Deaven, L. Gandin, M. Iredell, S. Saha, G. White, J. Woollen, Y. Zhu, A. Leetmaa, R. Reynolds, M. Chelliah, W. Ebisuzaki, W. Higgins, J. Janowiak, K. C. Mo, C. Ropelewski, J. Wang, R. Jenne, and D. Joseph, ‘The NCEP/NCAR 40-year reanalysis project’, *Bull. Amer. Meteor. Soc.*, **77**, 437–471 (1996).
- [60] R. Gibson, P. Källberg, and S. Uppala, ‘The ECMWF re-analysis (ERA) project’, *ECSN Newsletter*, **5**, 11–21 (1997).
- [61] S. D. Schubert, R. B. Rood, and J. Pfaffenberger, ‘An assimilated dataset for earth science applications’, *Bull. Amer. Meteor. Soc.*, **74**, 2331–2342 (1993).

- [62] E. L. Petersen, N. G. Mortensen, L. Landberg, J. Højstrup, and H. P. Frank, ‘Wind power meteorology. Part I: climate and turbulence’, *Wind Energy*, pilot issue, ??–?? (1998).
- [63] N. E. Busch, O. Christensen, L. Kristensen, L. Lading and S. E. Larsen, ‘Cups, vanes, propellers and laser anemometers’, *Air-Sea Interaction – Instruments and Methods*, Plenum Press, New York 1980, pp. 11–46.
- [64] L. Kristensen, ‘Cup anemometer behavior in turbulent environments’, *J. Atmos. Ocean. Techn.*, **15**, 5–17 (1998).
- [65] N. G. Mortensen, ‘Wind measurements for wind energy applications – a review’, *Wind Energy Conversion 1994. Proceedings of the 16th British Wind Energy Association Conference*, Stirling, June 15–17, 1994, pp. 353–360.
- [66] B. M. Pedersen, K. S. Hansen, S. Øye, M. Brinch and O. Fabian, ‘Some experimental investigations on the influence of the mounting arrangements on the accuracy of cup-anemometer measurements’, *J. Wind. Eng. Ind. Aerodyn.*, **39**, 373–383 (1992).
- [67] C. Kraan and W. A. Oost, ‘A new way of anemometer calibration and its application to a sonic anemometer’, *J. Atmos. Ocean. Tech.*, **6**, 516–524 (1989).
- [68] N. G. Mortensen, *Flow-response characteristics of the Kaijo Denki omnidirectional sonic anemometer (DAT 300/TR-61B)*, Risø-R-704(EN), Risø National Laboratory, Roskilde, Denmark 1994.
- [69] A. Grelle and A. Lindroth, ‘Flow distortion by a Solent sonic anemometer: wind tunnel calibration and its assessment for flux measurements over forest and field’, *J. Atmos. Ocean. Tech.*, **11**, 1529–1542 (1994).
- [70] N. G. Mortensen and J. Højstrup, ‘The Solent sonic – response and associated errors’, *Ninth Symposium on Meteorological Observations and Instrumentation*, Charlotte, NC, March 27–31, 501–506, 1995.
- [71] Källstrand, B. ‘Low level jets in the Baltic Sea area’, *Proceedings of the European Wind Energy Conference*, Dublin, Ireland, 6–9 October 1997, pp. 381–384.
- [72] J. Højstrup, E. L. Petersen, L. Landberg, R. J. Barthelmie, K. Bumke, U. Krager, L. Hasse, A. S. Smedman, H. Bergström, G. Adrian, F. Fiedler, B. Tammelin, *Baltic Sea Wind Resources*, Final report for Joule project, JOU2-CT93-0325, Risø report DOK-495, 1996.
- [73] H. Charnock, ‘Wind stress on a water surface’, *Q. J. R. Meteorol. Soc.*, **81**, 639–640 (1955).
- [74] H. K. Johnson, J. Højstrup, H. J. Vested and S. E. Larsen, S.E., ‘On the dependence of sea surface roughness on wind waves’, *J. Physical Oceanography*, **28**, 1702–1716 (1997).
- [75] J. Højstrup, *Meteorological measurements at Nibe, 1980–1992*, Report EEV 95–02, DEFU, Lyngby, Denmark 1995.
- [76] J. Højstrup, ‘Roughness lengths in coastal terrain’. *Proceedings from 11th Symposium on Boundary Layers and Turbulence*, Charlotte, NC, March 1995, pp. 481–484.
- [77] P. A. Taylor and J.R. Salmon, ‘A model for the correction of surface wind data for sheltering by upwind obstacles’, *J. Appl. Met.*, **32**, 1683–1694 (1993).
- [78] J. L. Walmsley, I. Troen, D. P. Lalas and P. J. Mason, ‘Surface-layer flow in complex terrain: Comparison of models and full-scale observations’, *Boundary-Layer Meteorol.*, **52**, 259–281 (1990).
- [79] A. J. Bowen, and N. G. Mortensen, ‘Exploring the limits of WASP: the Wind Atlas Analysis and Application Program’, *Proceedings of the 1996 European Union Wind Energy Conference*, Göteborg, Sweden, 20–24 May, 1996, pp. 584–587.
- [80] N. Wood, ‘The onset of separation in neutral, turbulent flow over hills’,

- Boundary-Layer Meteorol.*, **76**, 137–164 (1995).
- [81] N. G. Mortensen and E. L. Petersen, ‘Influence of topographical input data on the accuracy of wind flow modelling in complex terrain’, *Proceedings of the European Wind Energy Conference*, Dublin, Ireland, 6–9 October 1997, pp. 317–320.
 - [82] S. Finardi, G. Brusasca, M. G. Morselli, F. Trombetti, and F. Tampieri, ‘Boundary-layer flow over analytical two-dimensional hills: A systematic comparison of different models with wind tunnel data’, *Boundary-Layer Meteorol.*, **63**, 259–291 (1993).
 - [83] G. Gross, ‘On the applicability of numerical mass-consistent wind field models’, *Boundary-Layer Meteorol.*, **77**, 379–394 (1996).
 - [84] J. C. R. Hunt, S. Leibovich, and K. J. Richards, ‘Turbulent shear flow over low hills’, *Q. J. R. Meteorol. Soc.*, **114**, 1435–1470 (1988).
 - [85] G. Adrian and F. Fiedler, ‘Simulation of unstationary wind and temperature fields over complex terrain and comparison with observations’, *Beitr. Phys. Atmosph.*, **64**, 27–48 (1991).
 - [86] G. Adrian, *Zur Dynamik des Windfeldes über orographisch gegliedertem Gelände*, Ber. Deutschen Wetterdienstes 188, Offenbach am Main 1994. 142 pp.
 - [87] F. Frey-Buness, D. Heimann, and R. Sausen, ‘A statistical-dynamical downscaling procedure for global climate simulations’, *Theor. Appl. Climatol.*, **50**, 117–131 (1995).
 - [88] H. P. Frank and L. Landberg, ‘Modelling the wind climate of Ireland’. *Boundary-Layer Meteorol.*, **85**, 359–378 (1997).
 - [89] H. P. Frank and L. Landberg, ‘Numerical simulation of the Irish wind climate and comparison with wind atlas data’, *Proceedings of the European Wind Energy Conference*, Dublin, Ireland, 6–9 October 1997, pp. 309–312.
 - [90] L. Landberg and S. J. Watson, ‘Short-term prediction of local wind conditions’, *Boundary-Layer Meteorol.*, **70**, 171–195 (1994).
 - [91] L. Landberg, ‘Short-term prediction of the power production from wind farms’, *J. Wind. Eng. Ind. Aerodyn.*, **80**, 207–220 (1999).
 - [92] B. Machenhauer (ed.), *HIRLAM final report*. HIRLAM Technical Report 5, Danish Meteorological Institute, Copenhagen, Denmark 1988.
 - [93] P. Sanderhoff, *PARK – User’s Guide. A PC-program for calculation of wind turbine park performance*, Risø-I-668(EN), Risø National Laboratory, Roskilde, Denmark 1993.
 - [94] L. Landberg, M. A. Hansen, K. Vesterager, W. Bergstrøm, *Implementing Wind Forecasting at a Utility*, Risø-R-929(EN), Risø National Laboratory, Roskilde, Denmark 1997.
 - [95] P. D. Andersen, E. L. Petersen, P. H. Jensen, J. Beurskens, G. Elliot, J. P. Molly, ‘Wind Energy’, *The Future of Renewable Energy*, EUREC Agency, James & James (Science Publishers) Ltd, London 1996, pp. 154–183.
 - [96] H. F. Diaz, K. Wolter and S. D. Woodruff, *Proceedings of the International COADS Workshop*, Boulder, CO, January 1992, 390 pp.

Bibliographic Data Sheet

Risø-I-1206(EN)

Title and author(s)

Wind Power Meteorology

Erik L. Petersen, Niels G. Mortensen, Lars Landberg, Jørgen Højstrup and Helmut P. Frank

Dept. or group Date
Wind Energy Department December 1997

Groups own reg. number(s) Project/contract No.

VKM 04820-00

Pages	Tables	Illustrations	References
45	1	23	96

Abstract (Max. 2000 char.)

Wind power meteorology has evolved as an applied science, firmly founded on boundary-layer meteorology, but with strong links to climatology and geography. It concerns itself with three main areas: siting of wind turbines, regional wind resource assessment, and short-term prediction of the wind resource. The history, status and perspectives of wind power meteorology are presented, with emphasis on physical considerations and on its practical application. Following a global view of the wind resource, the elements of boundary layer meteorology which are most important for wind energy are reviewed: wind profiles and shear, turbulence and gust, and extreme winds.

The data used in wind power meteorology stem mainly from three sources: on-site wind measurements, the synoptic networks, and the re-analysis projects. Wind climate analysis, wind resource estimation and siting further require a detailed description of the topography of the terrain – with respect to the roughness of the surface, near-by obstacles, and orographical features. Finally, the meteorological models used for estimation and prediction of the wind are described; their classification, inputs, limitations and requirements. A comprehensive modelling concept, meso/micro-scale modelling, is introduced and a procedure for short-term prediction of the wind resource is described.

Copies to:

Risø Library (2)